A Comparative Linear Buckling Analysis of Different Isotropic Plates with and without Stiffeners for Different Boundary Conditions

Course No.: NAME-400

Submitted By-

Mohammad Shah Miran
Student ID: 1612007

Mohammad Abrar Uddin
Student ID: 1612021

Md. Nafis Soumik
Student ID: 1612053

Submitted To-

Department of Naval Architecture and Marine Engineering
in partial fulfillment of the requirements for the degree of Bachelor of Science in Naval Architecture and Marine Engineering.

Supervised by-

Dr. Md. Shahidul Islam
Professor
Department of Naval Architecture and Marine Engineering

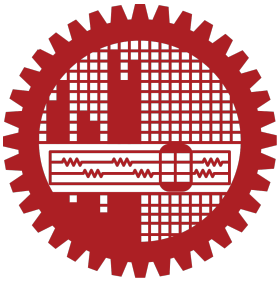

Bangladesh University of Engineering and Technology (BUET)
Dhaka-1000, Bangladesh
May , 2022

CERTIFICATION

This is to certify that the work presented in the thesis is an outcome of the investigation carried out by the authors under the supervision of Professor Dr. Md. Shahidul Islam, Department of Naval Architecture and Marine Engineering , Dhaka. It is declared that this thesis has been submitted only for the award of graduation.

Authors

Mohammad Shah Miran	Mohammad Abrar Uddin	Md. Nafis Soumik

Signature of the Supervisor

Dr. Md. Shahidul Islam

Professor
Department of Naval Architecture and Marine Engineering
Bangladesh University of Engineering and Technology (BUET)

ACKNOWLEDGMENTS

We would like to convey our heartfelt gratitude to our supervisor Dr. Md. Shahidul Islam for his guidance and support on this project showing us how to do good research and above all for being there as our mentor. He shared his wisdom with us in analyzing subject matters and at the same time valued our thinking approach to synthesize those topics. His suggestions and his reviews helped us in solving problems, and his support gave us strength at the time of our disappointment. We thank our friends and families who have been with us as well guiding our way.

ABSTRACT

Plate buckling problem is an active area of research in the shipbuilding industry.Generally physical structure of stiffened and unstiffened plates are subjected to compressive in-plane loading and a continuous increase of these load results in buckling which in terms causes structural failure. Linear buckling analysis predicts the theoretical buckling strength of an elastic structure. This dissertation investigates modelling and linear buckling analysis of stiffened and unstiffened rectangular isotropic plates for two different boundary conditions.The results are found out with the theoretical formulation and validated with simulation through a series of comparative studies in the finite element software ANSYS. Stiffeners of rectangular shape, L shape and T shape are used for a comparative analysis.

Keywords: Linear Buckling, Eigen value Buckling, Isotropic Material, Stiffened panel, Finite Element Analysis.

NOMENCLATURE

The following are the list of variables used in this thesis:

R Bracket radius

$\{T\}$ Traction force per unit area

t Thickness of the plate

∇ Laplacian operator

U Strain energy

$\{E\}$ Young's Modulus

t Specimen depth

y Distance of point considered from neutral axis

$\{\varepsilon\}$ Normal strain

η Natural coordinate

ξ Natural coordinate

Π Potential energy

N_x Buckling load

K_c buckling coefficient

σ_i Normal stress

σ_{ij} Shear stress

ϵ_i Normal strain

ϵ_{ij} Shear strain

$\sigma_{\max}$ Maximum stress

M_i Moment about i axis

M_{ij} Moment about ij plane

N_i Normal force along i axis

N_{ij} Normal force about ij plane

Q_i Shear force along i axis

Q_{ij} Shear force about ij plane

G $Shear Modulus$

D plate flexural stiffness per unit width

ν Poisson's ratio

TABLE OF CONTENTS

LIST OF TABLES

LIST OF FIGURES

CHAPTER 1

INTRODUCTION

The loss of a plate's stability under compressive loading is known as buckling. Loss of stability means that the shape of the buckled structure changes into a different configuration when the loads reach a critical value. Buckling occurrence depends on the shape of the structure, properties of the material, loading configuration and boundary conditions. Different bodies buckle in different ways. Flat plates experience bifurcation buckling, also known as classical buckling. Buckling occurs when thin walled or un-stiffened structures are subjected to various forms of loads such as uniaxial compression, biaxial compression, bending moment, and so on. Most thin walled structures in engineering constructions are stiffened for structural efficiency and weight conservation without sacrificing strength.

Ships experience buckling on various locations. The collapse of the deck structure of a ship hull girder can occur as a result of the induced high compressive stress by sagging bending moment exceeding the ultimate buckling strength of deck plating.[13]

The most frequent technique to improve the buckling resistance of an un-stiffened structure is to increase its thickness or use stiffeners. In most circumstances, the decision is based on overall cost, which is the cost of increasing the web thickness of an un-stiffened structure, which results in a heavier product. Reinforcing the thin-walled construction using light-weight stiffeners, on the other hand, lowers both the cost and the weight. The most important considerations for designers are light weight structural performance and efficiency. As a result, high-performance items must be lightweight while also being strong enough to withstand extreme loading conditions. Instead of increasing the thickness of an un-stiffened structure to prevent buckling, the recommended method is to apply a stiffener or stiffeners.

To solve the problem of plate buckling, many analysis approaches have been offered. In structural engineering, Finite Element Analysis (FEA) is one of the most often used methods. Its capacity to analyse complex geometries and contain nonlinearities owes to its extensive theory. The Finite Element software ANSYS will be used to perform the required analysis.

1.1 Objective

- To find the linear buckling behaviour for isotropic plates of different materials with simply supported edges (SSSS) and Clamped edges (CCCC) as the boundary conditions.
- Stiffeners of rectangular shape, T shape and L shape and their effects on linear buckling behaviour of the similar plates with stiffeners for the simply supported boundary condition are studied.
- To compare the results obtained in the analysis with theoretical results.
- To compare which type of stiffener provides the better resistance to buckling.

1.2 Basic Concepts

1.2.1 Isotropic Material

Isotropic materials have properties that do not change when tested in different directions. Isotropic materials differ from anisotropic materials, which have different properties depending on the direction they are tested in. Glass, polymers, and metals are examples of isotropic materials. On the other hand, the word "homogeneous" refers to the uniformity of the structure of a particular substance. Homogeneity means the uniformity of structure and isotropic means the uniformity of physical properties.

1.2.2 Linear Buckling Analysis

Linear buckling is the most common and simple method of analysis. Linear-buckling analysis computes buckling load magnitudes and associated buckling modes. FEA programs can calculate a large number of buckling modes as well as the corresponding buckling-load factors (BLF). The BLF is expressed as a value that must be multiplied (or divided – depending on the FEA application) by the applied load to obtain the buckling-load magnitude. The buckling mode describes the shape of the structure when it buckles in a specific mode, but it does not provide the numerical values of the displacements or stresses. The numerical numbers can be shown, but they are just relative. This is in close analogy to modal analysis, which calculates the natural frequency and provides qualitative information on the modes of vibration (modal shapes), but not on the actual magnitude of displacements.

Theoretically, the number of buckling modes can be calculated as many times as the number of degrees of freedom in the FEA model. However, most of the time, only the initial positive buckling mode and its associated BLF are required to be found. This is due to the fact that higher buckling modes have no probability of occurring. Buckling almost always results in catastrophic failure or renders the structure useless. The nomenclature is termed as

the first positive buckling mode, because buckling modes are reported in the ascending order according to their numerical values. A buckling mode with a negative BLF means the load direction must be reversed (in addition to multiplying by the BLF magnitude) for buckling to happen. As a consequence of discretization error, linear buckling analysis overestimates the buckling load and provides nonconservative results. However, BLFs are also overestimated because of modelling errors. FE models most often represent geometry with no imperfections and loads and supports are applied with perfect accuracy with no offsets. In reality though, loads are always applied with offsets, faces are never perfectly flat, and supports are never perfectly rigid. Even if supports are modelled as flexible, their stiffness is never evenly distributed. Imperfections are always present in the real world. Considering the combined effect of discretization error (a minor effect) and modelling error (a major effect), designers should interpret the results of linear buckling analysis with caution. The linear-buckling analysis only predicts the buckled shape and not the direction of buckling.

1.2.3 Critical Buckling Load

The critical load is the maximum load that can be applied without causing lateral deflection (buckling). The column or plate will deflect laterally if the load is larger than the critical load. The critical load causes the column or plate to be in an unstable condition of equilibrium. A load that exceeds the critical load causes the column or plate to buckle and fail. As the load exceeds the critical load, lateral deflections grow and the material may fail in various modes.

1.2.4 Shell Elements

Shell elements that are suitable to model rectangular plates are Shell181 and Shell281. Shell elements simulate the concept of plate/shell theories, which reduce the plate problem to surface model with strain/deformation assumptions through the thickness. The ANSYS structural shell components are based on the first-order shear-deformation theory (FSDT).

1.2.5 Boundary Conditions

Boundary of a plate, i.e. edge, may have free, clamped or simply supported boundary conditions. Other less common boundary conditions include hinged, fixed and sliding edges. For buckling analysis, boundary conditions have to allow displacement at least in the direction in which load acts. Main boundary conditions of a plate under buckling analysis should be interpreted as follows:

(a) **Free edge (F):** It is not geometrically restrained in any way.

(b) **Simply supported edge (SS):** It is free to have in-plane displacements and rotates freely about its axis. This is the basic meaning of simply supported edges. Additional conditions

might be added to this boundary condition, like being inextensible or immovable, also called SS-1 and SS-2, respectively.

(c) **Clamped edge (C):** It is free to have only in-plane displacements.

(d) **Fixed edge:** It is a fully restrained edge. Neither rotations nor displacements are allowed.

1.3 Literature Review

1.3.1 Global (or overall) Buckling of Stiffened Plates

Many researchers have become interested in the analysis of stiffened plates. Several methods for predicting the global buckling load of stiffened plates have been proposed. Orthotropic plate theory [4] [12] is a convenient method for analyzing stiffened plates. This method is used to analyze stiffened plates subjected to lateral or in-plane loads. The method's philosophy is to smear out the stiffener in order to convert the stiffened plate into an equivalent plate of constant thickness.
Cox [3][11] investigated the initial buckling of longitudinal and transverse concentric plates with simply supported boundaries under uniaxial compression in 1954. In some cases, they developed a differential equation that operated under certain assumptions, while in others, they used the Rayleigh-Ritz method. They demonstrated the results for panels with two or three concentric stiffeners. Due to the complications introduced in interpreting the results, they ignored the torsional stiffener of the stringers in their analysis. The orthotropic plate approach was used by Hoppmann et al. [8] and Hoppmann and Baltimore [6] to analyze simply supported orthogonally stiffened plates under static and dynamic loading. The rigidities of the plates were determined experimentally.

Soper [15] used Levy's approach to present a large deflection analysis for laterally loaded orthotropic plates. He used a trigonometric series to approximate the stress functions and then solved the resulting set of non-linear equations numerically. He presented numerical results for edges that were simply supported and clamped.

Maaskant [10] investigated the elastic, post-buckling behavior of simply supported, equally spaced, orthogonally stiffened plates using the orthotropic plate approach. Kagan and Kubo [14] proposed an elasto-plastic method for analyzing initially perfect, laterally loaded, orthogonally stiffened plates.

1.3.2 Local Stiffened Plate Buckling

Many design standards simplify the prediction of local buckling of single or multi-panel stiffened plates by assuming the plate and stiffener are hinged or clamped along their lines of intersection, thereby ignoring the interaction between plate and stiffener elements. The data reported in Refs [2] for these limiting boundary conditions are then used to calculate the local

buckling response. The simply supported condition assumes that the attached stiffeners have zero rotational stiffness, whereas the clamped condition assumes an infinite value. In reality, the stiffeners have a finite rotation capacity, posing a middle case. Furthermore, little emphasis is placed on the treatment of the in-plane lateral restraint, from which destabilizing stresses develop, lowering the plate's local buckling stress.

1.4 Research Methodology

Finite Element Analysis software ANSYS have been used for Buckling Analysis in this study. Amongst the different element types in this software, SHELL281 element as shown in figure 1.1 has been used. The reason to choose this type of element is as follows:

- Through SHELL281, it is suitable to analyse thin to moderately thick structures.
- SHELL281 element is well suited for large rotations.
- SHELL281 element has 6 degrees of freedom.
- It is suitable for nonlinear large strains and linear applications.

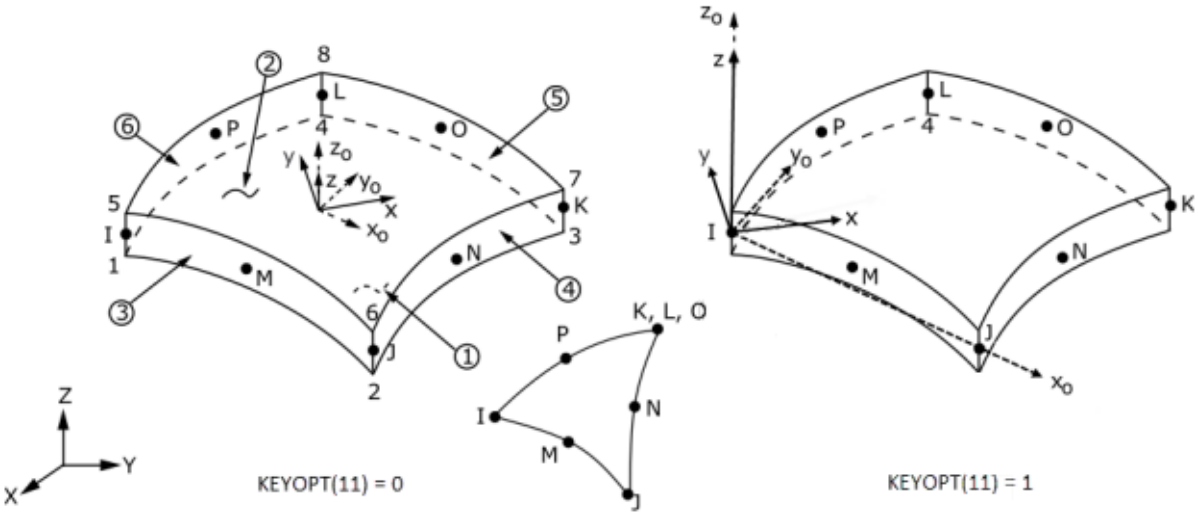

Figure 1.1: SHELL281 Element Geometry

A homogeneous and isotropic plate has been used initially to perform the analysis in the ANSYS software to converge the mesh as well as to validate the loading and boundary condition procedure used to predict the buckling load. The critical buckling load result is compared to the theoretical value and the mesh numbers are increased until the results converge. After obtaining a fixed element size to be used for meshing, the same loading case and boundary conditions are used for the other types of isotropic plates. The Plates have been analysed for two different boundary conditions in a sequential order. These boundary conditions include:

- All edges Simply Supported (SSSS)
- All Edges Clamped (CCCC)

The results obtained in the simulation are then compared with the theoretical results for validation. After this, the same loading case and simply supported boundary condition has been followed for three different types of stiffened plates of the same materials. Stiffeners of L shape, T shape and Box shaped were used. In case of stiffened plates, the work principle approach has been used. The general shape function for rectangular plates has been taken from Taylor-McLaurin's series upto fourth order. This has been used to derive the formulation of the governing Equation. By the formulated stability equations for different stiffeners, the theoretical value of the critical buckling load for stiffened plates has been calculated for SSSS and CCCC boundary conditions. The results are validated with the simulation results and necessary comparisons are done.

CHAPTER 2

THEORETICAL FRAMEWORK

2.1 Equations of Linear Elasticity in Cartesian Coordinates

2.1.1 Derivation of Equilibrium Equations in Control Volume

A material point within an elastic body can be acted on by two types of forces: body forces (F_i) and surface traction. The former are forces which are proportional to the mass, such as magnetic forces. Because the material is homogeneous, the body forces can be considered to be proportional to the volume. The latter involve stresses caused by neighboring control elements.

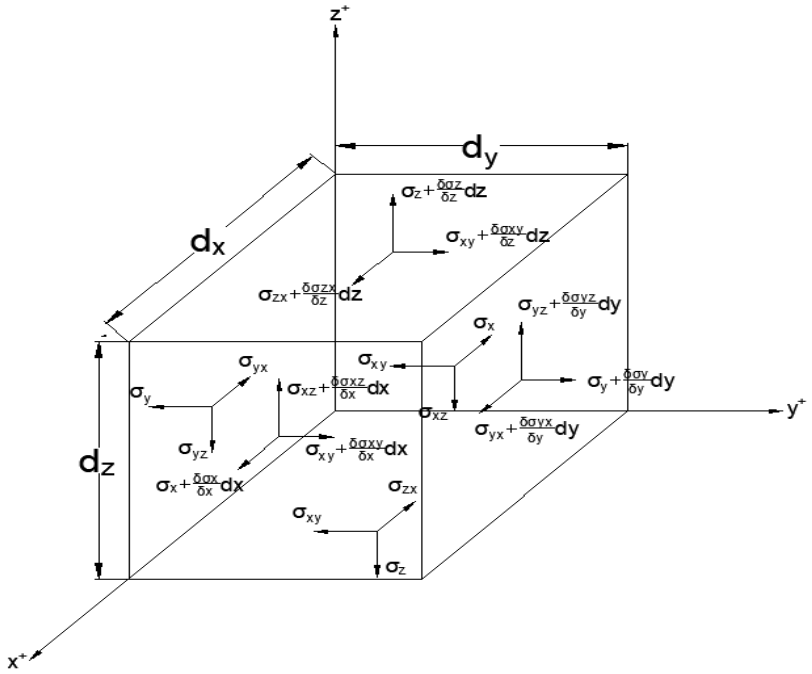

Figure 2.1: Control element showing variation of stresses.

Two types of forces-Body forces and Surface Traction act within a material point within an elastic body. As the material is homogeneous, the body forces can be considered proportional

to the volume. Now if we consider a control element as shown in Figure 2.1, the summation of forces in the X, Y and Z directions are given by:

$$\begin{aligned}&\left(\sigma_x+\frac{\partial\sigma_x}{\partial x}dx\right)dydz+\left(\sigma_{yx}+\frac{\partial\sigma_{yx}}{\partial y}\right)dxdz+\left(\sigma_{zx}+\frac{\partial\sigma_{zx}}{\partial z}dz\right)dxdy\\&-\sigma_x dydz-\sigma_{yx}dxdz-\sigma_{zx}dxdy+F_x dxdydz=0\end{aligned}\tag{2.1}$$

After cancellations, every term is multiplied by the volume, which upon division by the volume, results in

$$\frac{\partial\sigma_x}{\partial x}+\frac{\partial\sigma_{yx}}{\partial y}+\frac{\partial\sigma_{zx}}{\partial z}+F_x=0\tag{2.2}$$

Likewise, in the y and z direction, the equilibrium Equations are:

$$\frac{\partial\sigma_{xy}}{\partial x}+\frac{\partial\sigma_y}{\partial y}+\frac{\partial\sigma_{zy}}{\partial z}+F_y=0\tag{2.3}$$

$$\frac{\partial\sigma_{xz}}{\partial x}+\frac{\partial\sigma_{yz}}{\partial y}+\frac{\partial\sigma_z}{\partial z}+F_z=0\tag{2.4}$$

In the compact Einsteinian notation, the above three equilibrium Equations are written as: Likewise, in the y and z direction, the equilibrium Equations are:

$$\sigma_{ki}+F_i=0(i,k=x,y,z)\tag{2.5}$$

where this is the ith Equation, and the repeated subscripts k refer to each term being repeated in x, y and z, and where the comma means partial differentiation with respect to the subsequent subscript.

2.1.2 Stress-Strain Relations:

The mathematical relationship between stresses and strains at a material point in a three-dimensional body describes how the elastic material behaves. They are commonly referred to as constitutive Equations and are as follows:

$$\varepsilon_x=\frac{1}{E}\left[\sigma_x-\nu\left(\sigma_y+\sigma_z\right)\right]\tag{2.6}$$

$$\varepsilon_y=\frac{1}{E}\left[\sigma_y-\nu\left(\sigma_x+\sigma_z\right)\right]\tag{2.7}$$

$$\varepsilon_z=\frac{1}{E}\left[\sigma_z-\nu\left(\sigma_x+\sigma_y\right)\right]\tag{2.8}$$

$$\varepsilon_{xy}=\frac{1}{2G}\sigma_{xy}\tag{2.9}$$

$$\varepsilon_{yz}=\frac{1}{2G}\sigma_{yz}\tag{2.10}$$

$$\varepsilon_{zx}=\frac{1}{2G}\sigma_{zx}\tag{2.11}$$

In the compact Einsteinian notation, the above six Equations can be written as

$$\varepsilon_{ij}=a_{ijkl}\sigma_{kl}\tag{2.12}$$

where a_{ijk} is the generalised compliance tensor.

2.1.3 Linear Strain-Displacement Relations:

The strain-displacement relations are the kinematic equations relating the displacements that result from an elastic body being strained due to applied loads, or the strains that occur in the material when an elastic body is physically displaced.

$$\varepsilon_x = \frac{\partial u}{\partial x} \varepsilon_y = \frac{\partial v}{\partial y} \quad \varepsilon_z = \frac{\partial w}{\partial z} \tag{2.13}$$

$$\varepsilon_{xy} = \frac{1}{2}\left(\frac{\partial u}{\partial y} + \frac{\partial v}{\partial x}\right) \tag{2.14}$$

$$\varepsilon_{xz} = \frac{1}{2}\left(\frac{\partial u}{\partial z} + \frac{\partial w}{\partial x}\right) \tag{2.15}$$

$$\varepsilon_{yz} = \frac{1}{2}\left(\frac{\partial v}{\partial z} + \frac{\partial w}{\partial y}\right) \tag{2.16}$$

In compact Einsteinian notation, these six Equations are written as:

$$\varepsilon_{ij} = \frac{1}{2}\left(u_{i,j} + u_{j,i}\right) \quad (i, j = x, y, z) \tag{2.17}$$

2.1.4 Compatibility Equations:

The purpose of the compatibility equations is to ensure that the displacements of an elastic body are single-valued and continuous. They can be written as:

$$\frac{\partial^2 \varepsilon_{xx}}{\partial y \partial z} = \frac{\partial}{\partial x}\left(-\frac{\partial \epsilon_{yz}}{\partial x} + \frac{\partial \varepsilon_{zx}}{\partial y} + \frac{\partial \varepsilon_{xy}}{\partial z}\right) \tag{2.18}$$

$$\frac{\partial^2 \varepsilon_{yy}}{\partial z \partial x} = \frac{\partial}{\partial y}\left(-\frac{\partial \epsilon_{zx}}{\partial y} + \frac{\partial \varepsilon_{xy}}{\partial z} + \frac{\partial \varepsilon_{yz}}{\partial x}\right) \tag{2.19}$$

$$\frac{\partial^2 \varepsilon_{zz}}{\partial x \partial y} = \frac{\partial}{\partial z}\left(-\frac{\partial \epsilon_{xy}}{\partial z} + \frac{\partial \varepsilon_{yz}}{\partial x} + \frac{\partial \varepsilon_{zx}}{\partial y}\right) \tag{2.20}$$

$$2\frac{\partial^2 \varepsilon_{xy}}{\partial x \partial y} = \frac{\partial^2 \varepsilon_{xx}}{\partial y^2} + \frac{\partial^2 \varepsilon_{yy}}{\partial x^2} \tag{2.21}$$

$$2\frac{\partial^2 \varepsilon_{yz}}{\partial y \partial z} = \frac{\partial^2 \varepsilon_{yy}}{\partial z^2} + \frac{\partial^2 \varepsilon_{zz}}{\partial y^2} \tag{2.22}$$

$$2\frac{\partial^2 \varepsilon_{zx}}{\partial z \partial x} = \frac{\partial^2 \varepsilon_{zz}}{\partial x^2} + \frac{\partial^2 \varepsilon_{xx}}{\partial z^2} \tag{2.23}$$

The compatibility Equations are written in compact Einsteinian notation as follows:

$$\varepsilon_{ij,kl} + \varepsilon_{kl,ij} - \varepsilon_{ik,jl} - \varepsilon_{jl,ik} = 0 \quad (i, j, k, l = x, y, z). \tag{2.24}$$

However, in all of what follows, namely treating plates and beams, the governing differential equations are invariably expressed in terms of displacements, and if the solutions are functions that are single-valued and continuous, the compatibility Equations are not required. It can be demonstrated that the stress and strain tensor quantities are symmetric, i.e.,

$$\sigma_{ij} = \sigma_{ji} \text{ and } \varepsilon_{ij} = \varepsilon_{ji} (i, j = x, y, z). \tag{2.25}$$

As a result, there are fifteen independent variables for the elastic solid: six stress components, six strain components, and three displacements. When compatibility is satisfied, there are fifteen Equations: three equilibrium Equations, six constitutive relations, and six strain-displacement Equations.

2.2 Governing Equations For Isotropic Rectangular Plates

2.2.1 Assumptions of Plate Theory:

There are a number of assumptions that must be made in order to reduce the three-dimensional elasticity equations to a two-dimensional set that can be solved in classical, linear thin plate theory. Consider an elastic body in Figure 2.2 where $0 \leq x \leq a$, $0 \leq y \leq b$, and $h/2 \leq z \leq h/2$, with $h \ll a$ and $h \ll b$.

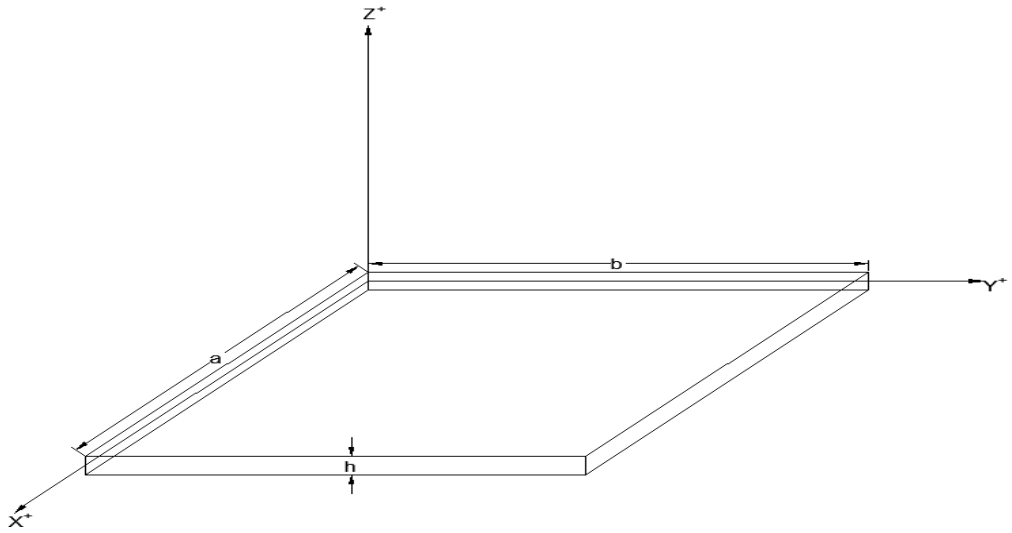

Figure 2.2: A simple rectangular plate

Now the following assumptions are being made.

1. In the unstressed state, a linear element of the plate extending through the thickness of the plate, normal to the mid surface, x-y plane:
   - is only rotated and translated in relation to the original coordinate system;
   - remains normal to the deformed middle surface.
2. A plate resists lateral and in-plane loads through bending, transverse shear stresses, and in-plane action, rather than block compression or tension in the thickness direction. This assumption is based on the fact that $h/a \ll 1$ and $h/b \ll 1$ environment.

   From 1, the followings are implied:

3. A lineal element through the thickness does not elongate or contract.
4. The lineal element remains straight upon load application.

2.2.2 Derivation of the Equilibrium Equations for a Rectangular Plate:

When the plate is subjected to lateral and in-plane loads, Figure 2.3 shows the positive directions of stress quantities to be defined. The followings are the stress couples:

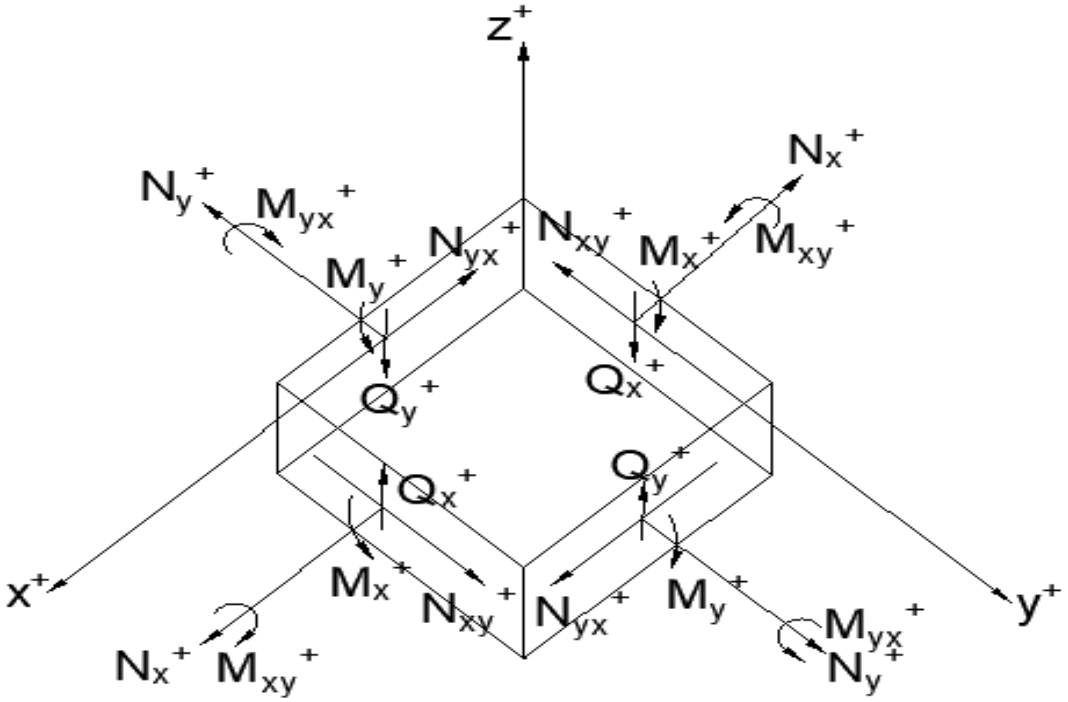

Figure 2.3: Positive directions of stress resultants and couples

$$M_x = \int_{\frac{-h}{2}}^{\frac{+h}{2}} \sigma_x Z x \tag{2.26}$$

$$M_y = \int_{\frac{-h}{2}}^{\frac{+h}{2}} \sigma_y z dz \tag{2.27}$$

$$M_{xy} = \int_{\frac{-h}{2}}^{\frac{+h}{2}} \sigma_{xy} Z\mathbb{Z} \tag{2.28}$$

$$M_{yx} = \int_{\frac{-h}{2}}^{\frac{+h}{2}} \sigma_{yx} Z z = M_{xy} \tag{2.29}$$

Similarly, the shear resultants are defined as,

$$Q_x = \int_{\frac{-h}{2}}^{\frac{+h}{2}} \sigma_{xz} \mathbb{Z} \tag{2.30}$$

$$Q_y = \int_{\frac{-h}{2}}^{\frac{+h}{2}} \sigma_{yz} \tag{2.31}$$

Again, the shear resultant is the physical sum of all shear stresses acting on all infinitesimal control elements across the thickness of the plate at the location in the thickness direction (x, y). Finally, the stress outcome variables are defined as:

$$N_x = \int_{-h/2}^{+h/2} \sigma_x \, dx \tag{2.32}$$

$$N_y = \int_{-h/2}^{+h/2} \sigma_y \, dz \tag{2.33}$$

$$N_{xy} = \int_{-h/2}^{+h/2} \sigma_{xy} \, dz \tag{2.34}$$

$$N_{yx} = \int_{-h/2}^{+h/2} \sigma_{yx} \, dz = N_{xy} \tag{2.35}$$

These are the total in-plane stresses acting on all infinitesimal control elements across the plate thickness at x, y. When integrating the stress quantities across the thickness h in plate theory, the details of each control element under consideration are ignored. Rather than considering stresses at each material point, the integrated stress quantities defined above are used. Performing certain integrations on the equations of elasticity to obtain the governing equations for plates is the procedure. Proceeding, multiply Equation 2.2 by $z \, dz$ and integrate between $-h/2$ and $+h/2$, as follows:

$$\int_{-h/2}^{+h/2} z\frac{\partial \sigma_x}{\partial x} + z\frac{\partial \sigma_{xy}}{\partial y} + z\frac{\partial \sigma_{xz}}{\partial z}\Big) dz = 0 \tag{2.36}$$

$$\frac{\partial}{\partial x}\int_{-h/2}^{+h/2} \sigma_x z \, dz + \frac{\partial}{\partial y}\int_{-h/2}^{+h/2} \sigma_{xy} z \, dz + \int_{-h/2}^{+h/2} z\frac{\partial \sigma_{xz}}{\partial z} \, dz = 0 \tag{2.37}$$

$$\left[\frac{\partial M_x}{\partial x} + \frac{\partial M_{xy}}{\partial y} + z\sigma_{xz}\right]_{-h/2}^{+h/2} - \int_{-h/2}^{+h/2} \sigma_{xz} \, dz = 0. \tag{2.38}$$

As x and z are orthogonal to one another, the order of differentiation and integration can be reversed. When there are no shear loads on the upper or lower plate surface, $\sigma_{xz} = \sigma_{zx} = 0$ is the third term. If there are surface shear stresses, define $\tau_{1x} = \sigma_{xz}(+h/2)$ and $\tau_{2x} = \sigma_{xz}(-h/2)$ to get the results shown in Equation 2.39. It should also be noted that for plates supported on an edge, σ_{xz} may not go to zero at $\pm h/2$, indicating that the theory is inaccurate at that edge, but the solutions are satisfactory away from the edge supports due to St. Venant's Principle.

$$\frac{\partial M_x}{\partial x} + \frac{\partial M_{xy}}{\partial y} + \frac{h}{2}(\tau_{1x} + \tau_{2x}) - Q_x = 0. \tag{2.39}$$

Likewise Equation 2.3 becomes

$$\frac{\partial M_{xy}}{\partial x} + \frac{\partial M_y}{\partial y} + \frac{h}{2}\left(\tau_{1y} + \tau_{2y}\right) - Q_y = 0 \tag{2.40}$$

where

$$\tau_{1y} = \sigma_{yz}(+h/2) \text{ and } \tau_{2y} = \sigma_{yz}(-h/2). \tag{2.41}$$

These two Equations describe the moment equilibrium of a plate element. Looking now at Equations 2.4, multiplying it by dz, and integrating between $-h/2$ and $+h/2$, results in

$$\int_{-h/2}^{+h/2}\left(\frac{\partial\sigma_{zx}}{\partial x}+\frac{\partial\sigma_{zy}}{\partial y}+\frac{\partial\sigma_z}{\partial z}\right)dz=0 \tag{2.42}$$

$$\frac{\partial Q_x}{\partial x}+\frac{\partial Q_y}{\partial y}+\sigma_z\int_{-h/2}^{+h/2}=0 \tag{2.43}$$

$$\frac{\partial Q_x}{\partial x}+\frac{\partial Q_y}{\partial y}+p_1(x,y)-p_2(x,y)=0 \tag{2.44}$$

where $p_1(x,y)=\sigma_z(+h/2)$, $p_2(x,y)=\sigma_z(-h/2)$. Equation 2.44 may also derived by considering vertical equilibrium of a plate element shown in Figure 2.4.

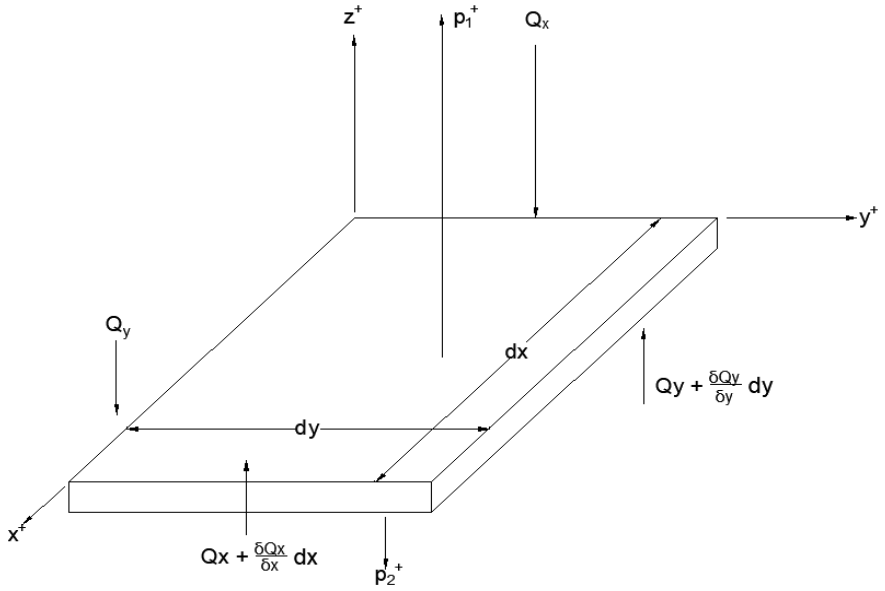

Figure 2.4: Vertical Forces on a Plate Element.

In terms of in-plane stress resultants and surface shear stresses, multiplying Equation 2.2 and Equation 2.3 by dz and integrating across the plate thickness yields the plate equilibrium Equations in the x and y directions, respectively.

$$\frac{\partial N_x}{\partial x}+\frac{\partial N_{xy}}{\partial y}+(\tau_{1x}-\tau_{2x})=0 \tag{2.45}$$

$$\frac{\partial N_{xy}}{\partial x}+\frac{\partial N_y}{\partial y}+\left(\tau_{1y}-\tau_{2y}\right)=0 \tag{2.46}$$

2.2.3 Derivation of Plate Moment-Curvature Relations and Integrated Stress Resultant-Displacement Relations

Now, the plate equations must be derived corresponding to the elastic stress strain relations. The strains , ϵ_x , ϵ_y and $\epsilon_x y$ will not be used explicitly since the stresses have been

averaged by integrating through the thickness. Hence, displacements are utilized. Thus, combining Equation 2.6 through Equation 2.17 gives the following, it is to be mentioned that σ_z has been assumed zero in the interior of the plate and excluding Equation 2.9 for reasons given previously.

$$\frac{\partial u}{\partial x} = \frac{1}{E}\left[\sigma_x - \upsilon\sigma_y\right] \tag{2.47}$$

$$\frac{\partial v}{\partial y} = \frac{1}{E}\left[\sigma_y - \upsilon\sigma_x\right] \tag{2.48}$$

$$\frac{1}{2}\left(\frac{\partial u}{\partial y} + \frac{\partial v}{\partial x}\right) = \frac{1}{2G}\sigma_{xy} \tag{2.49}$$

$$\frac{1}{2}\left(\frac{\partial v}{\partial z} + \frac{\partial w}{\partial y}\right) = \frac{1}{2G}\sigma_{yz} \tag{2.50}$$

$$\frac{1}{2}\left(\frac{\partial w}{\partial x} + \frac{\partial u}{\partial z}\right) = \frac{1}{2G}\sigma_{xz} \tag{2.51}$$

Now, From the admissible displacements resulting from the plate theory assumptions:

$$u = u_0(x,y) + z\bar{\alpha}(x,y) \tag{2.52}$$

$$v = v_0(x,y) + z\bar{\beta}(x,y) \tag{2.53}$$

$$w = w(x,y) \text{ only.} \tag{2.54}$$

A lineal element passing through the plate will experience translations and rotations but no extensions or contractions, according to plate theory. The lateral deflections must be small in comparison to the plate thickness for these assumptions to be valid. It should be noted that if a plate is very thin, lateral loads can cause lateral deflections many times its thickness, and the plate then behaves largely as a membrane due to its lack of bending resistance, i.e., $D \to 0$.

Transverse shear deformation must be zero according to classical plate theory assumptions.If $\varepsilon_{xz} = \varepsilon_{yz} = 0$, then from Equation 2.15 and Equation 2.16:

$$\frac{1}{2}\left(\frac{\partial u}{\partial z} + \frac{\partial w}{\partial x}\right) = 0, or \frac{\partial u}{\partial z} = -\frac{\partial w}{\partial x},$$

Likewise,

$$\frac{\partial v}{\partial z} = -\frac{\partial w}{\partial y}$$

Hence, from Equation 2.52 through Equation 2.54 and the above, it is seen that the rotations are:

$$\bar{\alpha} = -\frac{\partial w}{\partial x} \tag{2.55}$$

$$\bar{\beta} = -\frac{\partial w}{\partial y} \tag{2.56}$$

Using Equation 2.52 and Equation 2.47, multiplying Equation 2.47 through by $z\,dz$ and integrating from $-h/2$ to $+h/2$, one obtains

$$\int_{-h/2}^{+h/2} \frac{\partial u_0}{\partial x} z\,dz + \int_{-h/2}^{+h/2} z^2 \frac{\partial \bar{\alpha}}{\partial x}\,dz = \int_{-h/2}^{+h/2} \frac{1}{E}\left[\sigma_x - \nu\sigma_y\right] z\,dz. \tag{2.57}$$

Likewise Equation 2.53 and Equation 2.48 result in

$$\int_{-h/2}^{+h/2} \frac{\partial v_0}{\partial y} z\,dz + \int_{-h/2}^{+h/2} z^2 \frac{\partial \bar{\beta}}{\partial y}\,dz = \int_{-h/2}^{+h/2} \frac{1}{E}\left[\sigma_y - \nu\sigma_x\right] z\,dz \tag{2.58}$$

and Equation 2.52, Equation 2.53 and Equation 2.49 give:

$$\int_{-h/2}^{+h/2} \left(\frac{\partial u_0}{\partial y} + \frac{\partial v_0}{\partial x}\right) z\,dz + \int_{-h/2}^{+h/2} \left(z^2 \frac{\partial \bar{\alpha}}{\partial y} + z^2 \frac{\partial \bar{\beta}}{\partial x}\right) dz = \int_{-h/2}^{+h/2} \frac{1}{G}\sigma_{xy} z\,dz \tag{2.59}$$

Integrating Equation 2.57,Equation 2.58 and Equation 2.59, and then incorporating in Equation 2.55 and Equation 2.56:

$$\frac{h^3}{12}\frac{\partial \bar{\alpha}}{\partial x} = \frac{1}{E}\left[M_x - \nu M_y\right] = -\frac{h^3}{12}\frac{\partial^2 w}{\partial x^2} \tag{2.60}$$

$$\frac{h^3}{12}\frac{\partial \bar{\beta}}{\partial y} = \frac{1}{E}\left[M_y - \nu M_x\right] = -\frac{h^3}{12}\frac{\partial^2 w}{\partial y^2} \tag{2.61}$$

$$\frac{h^3}{12}\left(\frac{\partial \bar{\alpha}}{\partial y} + \frac{\partial \bar{\beta}}{\partial x}\right) = \frac{1}{G} M_{xy} = -\frac{h^3}{6}\frac{\partial^2 w}{\partial x \partial y} \tag{2.62}$$

Since, $G = E/2(1+\nu)$

$$M_{xy} = -(1-\nu) D \frac{\partial^2 w}{\partial x \partial y} \text{ where } D = \frac{E h^3}{12\left(1-\nu^2\right)}. \tag{2.63}$$

Solving Equation 2.57 and Equation 2.58 for M_x and M_y results in:

$$M_x = -D\left[\frac{\partial^2 w}{\partial x^2} + \nu \frac{\partial^2 w}{\partial y^2}\right] \tag{2.64}$$

$$M_y = -D \cdot \frac{\partial^2 w}{\partial y^2} + \nu \frac{\partial^2 w}{\partial x^2}\Bigg] \tag{2.65}$$

The moment-curvature relations are defined as Equation 2.63 through Equation 2.65, with D representing the plate's flexural stiffness per unit width. The curvatures in these moment-curvature relations for classical theory are as follows:

$$\kappa_x = \frac{\partial \bar{\alpha}}{\partial x} = -\frac{\partial^2 w}{\partial x^2}, \quad \kappa_y = \frac{\partial \bar{\beta}}{\partial y} = -\frac{\partial^2 w}{\partial y^2} \tag{2.66}$$

$$\kappa_{xy} = \left(\frac{\partial \bar{\alpha}}{\partial y} + \frac{\partial \bar{\beta}}{\partial x}\right) = -\frac{\partial^2 w}{\partial x \partial y}$$

Likewise, substituting Equation 2.64 and Equation 2.65 into Equation 2.39 and Equation 2.40 results in:

$$Q_x = -D\frac{\partial}{\partial x}\left(\nabla^2 w\right) + \frac{h}{2}\left(\tau_{1x} + \tau_{2x}\right) \tag{2.67}$$

$$Q_y = -D\frac{\partial}{\partial y}\left(\nabla^2 w\right) + \frac{h}{2}\left(\tau_{1y} + \tau_{2y}\right)$$

In the above, the two dimensional Laplacian operator ∇^2 is defined as follows:

$$\nabla^2 w = \frac{\partial^2 w}{\partial x^2} + \frac{\partial^2 w}{\partial y^2}.$$

The following integrated stress-strain relationships are obtained by substituting Equation 2.52 and Equation 2.53 into Equation 2.47 through Equation 2.49, multiplying the latter three Equations by dz, and integrating across the thickness:

$$N_x = K\left[\frac{\partial u_0}{\partial x} + \upsilon\frac{\partial v_0}{\partial y}\right] \tag{2.68}$$

$$N_y = K\left[\frac{\partial v_0}{\partial y} + \upsilon\frac{\partial u_0}{\partial x}\right] \tag{2.69}$$

$$N_{xy} = N_{yx} = Gh\left[\frac{\partial u_0}{\partial y} + \frac{\partial v_0}{\partial x}\right], \tag{2.70}$$

where, $Eh/\left(1-\upsilon^2\right) = K$, the plate extensional stiffness. Equation 2.68 through Equation 2.70 describe the in-plane force and deformation behavior.

2.2.4 Derivation of the Governing Differential Equations for a Plate

The equations governing the lateral deflections, and the bending and shearing action of a plate can be summarized as follows:

$$\frac{\partial M_x}{\partial x} + \frac{\partial M_{xy}}{\partial y} - Q_x + \frac{h}{2}(\tau_{1x} + \tau_{2x}) = 0 \tag{2.71}$$

$$\frac{\partial M_{xy}}{\partial x} + \frac{\partial M_y}{\partial y} - Q_y + \frac{h}{2}\left(\tau_{1y} + \tau_{2y}\right) = 0 \tag{2.72}$$

$$\frac{\partial Q_x}{\partial x} + \frac{\partial Q_y}{\partial y} + p_1 - p_2 = 0 \tag{2.73}$$

$$M_x = -D\left[\frac{\partial^2 w}{\partial x^2} + \nu\frac{\partial^2 w}{\partial y^2}\right] \tag{2.74}$$

$$M_y = -D\left[\frac{\partial^2 w}{\partial y^2} + \nu\frac{\partial^2 w}{\partial x^2}\right] \tag{2.75}$$

$$M_{xy} = -D(1-\nu)\frac{\partial^2 w}{\partial x \partial y} \tag{2.76}$$

The Equations governing the in-plane stress resultants and in-plane midsurface displacements are:

$$\frac{\partial N_x}{\partial x} + \frac{\partial N_{xy}}{\partial y} + (\tau_{1x} - \tau_{2x}) = 0 \tag{2.77}$$

$$\frac{\partial N_{xy}}{\partial x} + \frac{\partial N_y}{\partial y} + \left(\tau_{1y} - \tau_{2y}\right) = 0 \tag{2.78}$$

$$N_x = K\left[\frac{\partial u_0}{\partial x} + \nu\frac{\partial v_0}{\partial y}\right] \tag{2.79}$$

$$N_y = K\left[\frac{\partial v_0}{\partial y} + \nu\frac{\partial u_0}{\partial x}\right] \tag{2.80}$$

$$N_{xy} = Gh\left[\frac{\partial u_0}{\partial y} + \frac{\partial v_0}{\partial x}\right] \tag{2.81}$$

Equation 2.71 through Equation 2.81 are the eleven governing plate equations. As the plate can only tell the difference between normal tractions on the upper and lower surface. Thus, $p(x, y)$ can be defined as

$$p_1(x, y) - p_2(x, y) = p(x, y). \tag{2.82}$$

Substituting Equation 2.71 and Equation 2.72 into Equation 2.73 results in the following for the case of no shear stresses on the plate upper and lower surfaces:

$$\frac{\partial^2 M_x}{\partial x^2} + 2\frac{\partial^2 M_{xy}}{\partial x \partial y} + \frac{\partial^2 M_y}{\partial y^2} + p(x, y) = 0. \tag{2.83}$$

Substituting Equation 2.74 through Equation 2.76 into Equation 2.83 results in:

$$D\nabla^4 w = p(x, y), \tag{2.84}$$

where,

$$\nabla^2() = \frac{\partial^2()}{\partial x^2} + \frac{\partial^2()}{\partial y^2} \text{ and } \nabla^4() = \nabla^2\left(\nabla^2()\right).$$

The Laplacian operator, ∇^2, is the sum of the curvatures in two orthogonal directions at the plate location x, y. The biharmonic operator ∇^4 is the Laplacian of the Laplacian, and is thus physically the sum of the curvatures of the sum of the curvatures in orthogonal directions.

2.3 Buckling of Isotropic Plates

2.3.1 Derivation of the Plate Governing Equations for Buckling

The governing Equations for a thin plate under in-plane and lateral loads were previously derived. One governing Equation that described the relationship between lateral deflection and laterally distributed loading in those Equations is,

$$D\nabla^4 w = p(x, y) \tag{2.85}$$

and other Equations dealing with in-plane displacements, related to in-plane loads:

$$\nabla^4 u_0 = \nabla^4 v_0 = 0 \tag{2.86}$$

As previously stated, the Equation involving lateral displacements and loads are completely separate (uncoupled) from those involving in-plane loadings and displacements.

However, it is true that when in-plane loads are compressive, these compressive loads produce lateral displacements when they reach certain discrete values. Thus there is a coupling between in-plane loads and lateral displacements. As a result, a more comprehensive theory for this phenomenon, known as buckling or elastic instability, must be developed.

Unlike the development of the governing plate Equations in Section 2.2.4, which started with the three-dimensional equations of elasticity, the following section will start with an examination of the in-plane forces acting on a plate element, where the forces are assumed to be functions of the mid-surface coordinates x and y, as shown in Figure 2.5.

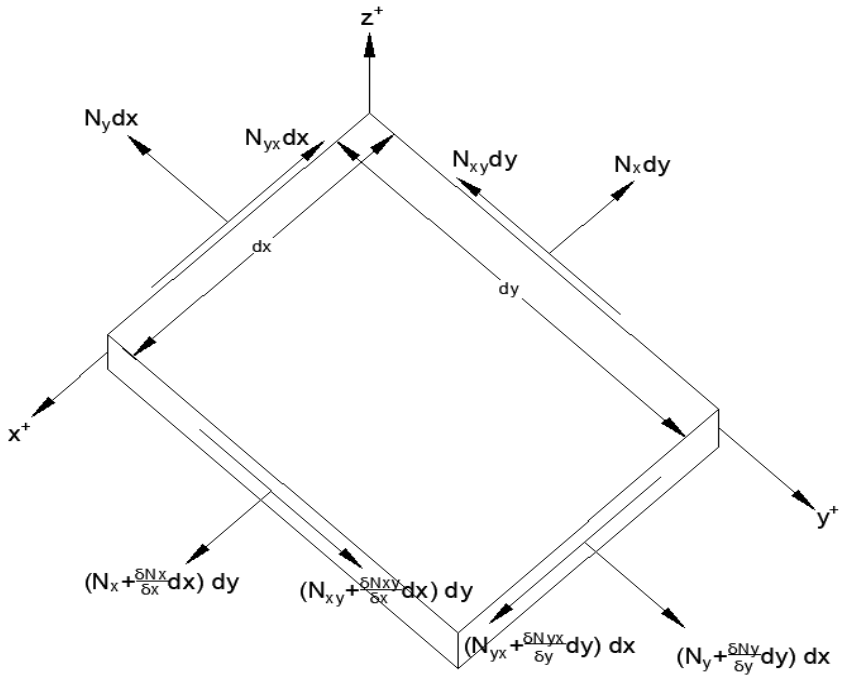

Figure 2.5: In-plane Forces on a Plate Element.

When the plate is subjected to both lateral and in-plane forces, i.e., when there is a lateral deflection, the relationship between forces and displacements is seen as shown in Figure 2.6,

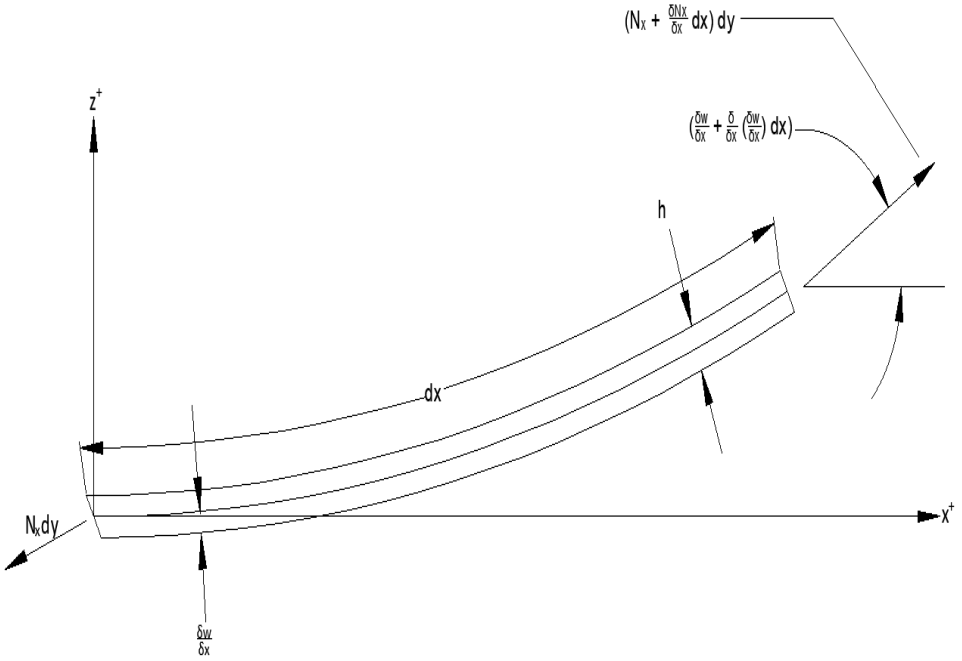

Figure 2.6: In-plane forces acting on a deflected plate element.

As a result, for small slopes, the z component of the Nx loading per unit area is:

$$\frac{1}{dx\,dy}\left[\left(N_x+\frac{\partial N_x}{\partial x}\,dx\right)dy\left(\frac{\partial w}{\partial x}+\frac{\partial^2 w}{\partial x^2}\,dx\right)-N_x\,dy\frac{\partial w}{\partial x}\right] \tag{2.87}$$

Neglecting terms of higher order, the force per unit area in the z direction is seen to be:

$$N_x \frac{\partial^2 w}{\partial x^2} + \frac{\partial N_x}{\partial x}\frac{\partial w}{\partial x} \tag{2.88}$$

Similarly, the z component of the N_y force per unit area is seen to be:

$$N_y \frac{\partial^2 w}{\partial y^2} + \frac{\partial N_y}{\partial y}\frac{\partial w}{\partial y} \tag{2.89}$$

Finally to investigate the z component of the in-plane resultants N_{xy} and N_{yx},
Hence, the z component per unit area of the in-plane shear resultant is:

(2.90)

$$\frac{1}{dx\,dy}\left\{\left(N_{xy} + \frac{\partial N_{xy}}{\partial x}\,dx\right)\left(\frac{\partial w}{\partial y} + \frac{\partial^2 w}{\partial x \partial y}\,dx\right)dy + (N_{yx} + \frac{\partial N_{yx}}{\partial y}\,dy\right)\left(\frac{\partial w}{\partial x} + \frac{\partial^2}{\partial x \partial y}\,dy\right)dx - N_{xy}\frac{\partial w}{\partial y}\,dy - N_{yx}\frac{\partial w}{\partial x}\,dx\right\}.$$

Neglecting higher order terms, this result in:

$$N_{xy}\frac{\partial^2 w}{\partial x \partial y} + \frac{\partial N_{xy}}{\partial x}\frac{\partial w}{\partial y} + N_{yx}\frac{\partial^2 w}{\partial x \partial y} + \frac{\partial N_{yx}}{\partial y}\frac{\partial w}{\partial x}. \tag{2.91}$$

The governing plate Equation can be modified to include the effect of these in-plane forces on the governing plate Equations using all of the above z components of forces per unit area.

$$D\nabla^4 w = p(x,y) + N_x\frac{\partial^2 w}{\partial x^2} + N_y\frac{\partial^2 w}{\partial y^2} + 2N_{xy}\frac{\partial^2 w}{\partial x \partial y} + \frac{\partial N_x}{\partial x}\frac{\partial w}{\partial x} + \frac{\partial N_y}{\partial y}\frac{\partial w}{\partial y} + \frac{\partial N_{xy}}{\partial x}\frac{\partial w}{\partial y} + \frac{\partial N_{yx}}{\partial y}\frac{\partial w}{\partial x} \tag{2.92}$$

However, from in-plane force equilibrium, it is remembered from Equation 2.45 and Equation 2.49, assuming no applied surface shear stresses that,

$$\frac{\partial N_x}{\partial x} + \frac{\partial N_{yx}}{\partial y} = 0, \tag{2.93}$$

$$\frac{\partial N_{xy}}{\partial x} + \frac{\partial N_y}{\partial y} = 0 \tag{2.94}$$

Substituting these into the expression above, the final form of the Equation is found to be:

$$D\nabla^4 w = p(x,y) + N_x\frac{\partial^2 w}{\partial x^2} + N_y\frac{\partial^2 w}{\partial y^2} + 2N_{xy}\frac{\partial^2 w}{\partial x \partial y} \tag{2.95}$$

2.3.2 Buckling of Isotropic Rectangular Plates Simply Supported on All Four Edges.

In the analysis of plates, Equation 2.95 should be used instead of Equation 2.85, whenever the in-plane forces are compressive and account for more than a few percent of the plate buckling loads. As the in-plane load that causes elastic stability is not dependent on a lateral load in the case of the plate, we will assume $p(x, y) = 0$ in Equation 2.95 to investigate the elastic stability.

As an example, consider a simply supported plate subjected to constant in-plane loads N_x and N_y (let $N_{xy} = 0$). Assume the Navier form for the solution of Equation 2.95

$$w(x, y) = \sum_{m=1}^{\infty} \sum_{n=1}^{\infty} A_{mn} \sin \frac{m\pi x}{a} \sin \frac{n\pi y}{b}. \tag{2.96}$$

By substituting Equation 2.96 for Equation 2.95, it is simple to define α as:

$$\alpha = N_y / N_x \tag{2.97}$$

The solution to the eigenvalue problem is found to be:

$$N_{x_{cr}} = -D\pi^2 \frac{\left[\left(\frac{m}{a}\right)^2 + \left(\frac{n}{b}\right)^2\right]^2}{\left[\left(\frac{m}{a}\right)^2 + \left(\frac{n}{b}\right)^2\right]} \tag{2.98}$$

The subscript cr indicates a critical load situation in which the plate buckles. Also note that in Equation 2.98 N_x is negative, indicating that the load is compressive.

The complete set of eigenvalues for the simply supported plate is given by Equation 2.98. Equation 2.95 has nontrivial solutions for these discrete values of N_x and N_y, where the lateral deflection is given by Equation 2.44; for other values $w(x, y) = 0$. The plate will buckle at the lowest buckling load (or eigenvalue) as the load increases, and the other eigenvalues have no physical meaning.

Defining the length to width ratio of the plate $r = a/b$, Equation 2.46 can be rewritten as:

$$N_x = -\frac{D\pi^2}{a^2} \frac{\left[m^2 + n^2 r^2\right]^2}{\left[m^2 + n^2 r^2 \alpha\right]}. \tag{2.99}$$

Now if in Equation 2.47, $\alpha = 0, r = 1$ and $m = n = 1$, then:

$$N_x = -\frac{4\pi^2 D}{a^2}. \tag{2.100}$$

It is to be mentioned that under any combination of N_x and/or N_y, a square plate simply

supported on all four edges will always buckle into a half sine wave (m = n = 1). Now, consider a plate that is only loaded in the x direction, with $N_y = 0$, and $\alpha = 0$. Equation 2.46 can be written as in this case as follows:

$$N_{x_{cr}} = -\frac{D\pi^2 a^2}{m^2}\left[\frac{m^2}{a^2} + \frac{n^2}{b^2}\right]^2 \tag{2.101}$$

The loaded plate is shown in Figure 2.7.

:

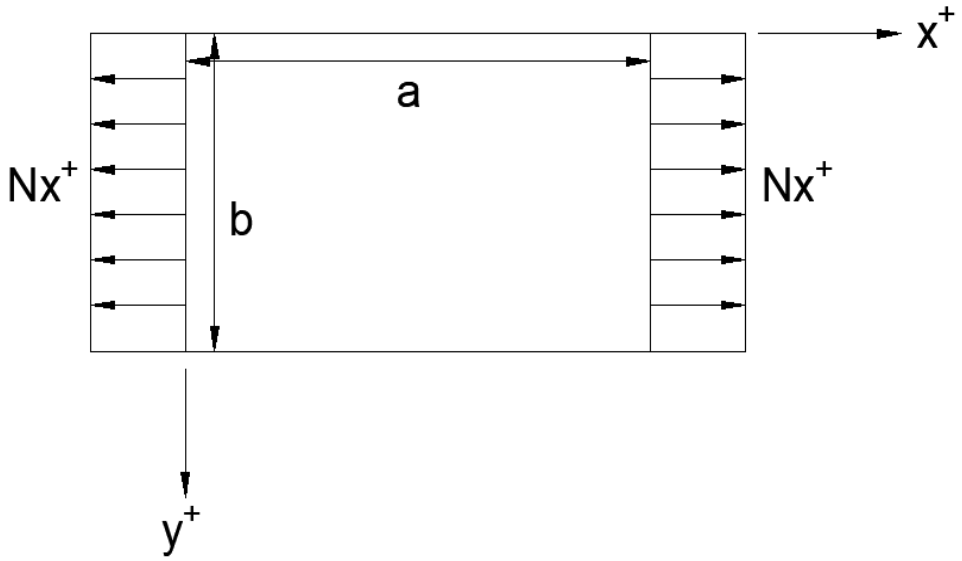

Figure 2.7: Plate Subjected to In-plane Load in the x Direction.

Equation 2.101 shows that the minimum values of N_x occur when n= 1, because n only appears in the numerator. Thus, regardless of the length or width of the plate, the buckling mode given by Equation 2.96 will always be one half sine wave [sin(y/b)] across the span for an isotropic plate simply supported on all four edges and subjected only to a uniaxial in-plane load. Since n = 1, Equation 2.101 can be written as,

$$\bar{N}_c = k_c \frac{\pi^2 D}{b^2} \tag{2.102}$$

where the buckling coefficient k_c is a function of both the plate aspect ratio a/b and the wavelength parameter

$$k_c = \left(\frac{mb}{a} + \frac{a}{mb}\right)^2 \tag{2.103}$$

The integer parameter m determines how many half waves will fit into the plate's length.

The wavelength parameter is unknown, but the aspect ratio a/b is known. Its value must be determined by visual inspection, which entails plotting the buckling coefficient as a function of a/b for successive values of the parameter m. Figure 2.8 depicts this phenomenon.

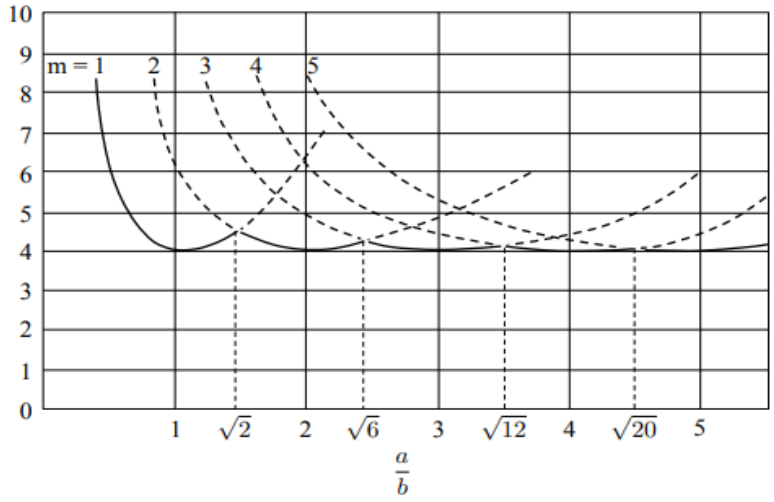

Figure 2.8: The buckling coefficient for a simply supported plate as a function of plate aspect ratio a/b and wave numbers.

2.3.3 Buckling of Isotropic Plates with Other Loads and Boundary Conditions

Simple displacement functions like Equation 2.96 do not exist for many other boundary conditions, and analytical, exact solutions analogous to Equation 2.98 and Equation 2.100 have not been found in some cases. In those cases, energy methods were used to find approximate solutions. Figure 2.9 depicts this phenomenon.

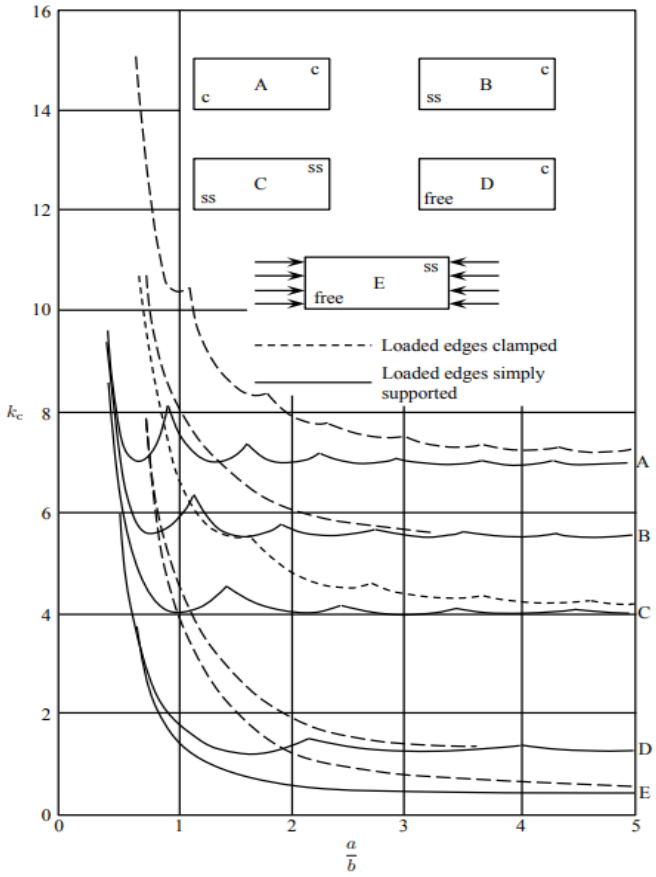

Figure 2.9: Effect of boundary conditions on the buckling coefficient of rectangular plates.[1]

2.4 Buckling of Isotropic stiffened panel

2.4.1 Stability of Plates Reinforced by Stiffener

The plate's stability can always be increased by increasing its thickness, but this design will be inefficient in terms of material weight. By keeping the plate thickness as small as possible and adding reinforcing stiffeners to increase stability, a more cost-effective solution can be achieved.

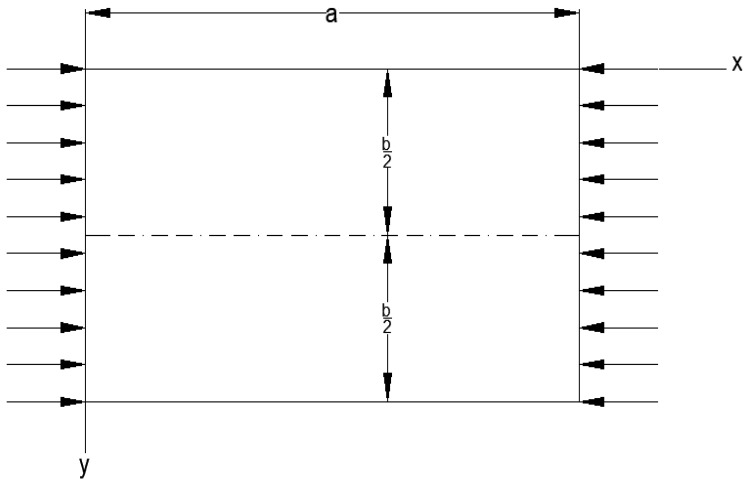

Figure 2.10: Plate with one stiffener.

By adding a longitudinal rib of suitable cross section that bisects the width of a compressed plate, as shown in Figure 2.10, its stability can be increased by about four times. The additional weight introduced by an adequate increase in plate thickness is usually much smaller than the weight of such a stiffener. In practical design, the proportions of reinforcing ribs should be such that the critical value of the stresses is equal to the material's yield-point stress. The strength of all of the materials is then maximized. The energy method can be used to determine the relationship between the cross-sectional dimensions of stiffeners and the critical value of stresses in a plate.

2.4.2 Governing Differential Equation of a stiffened rectangular panel

Consider a plate with length a, width b, and thickness t, as shown in Figure 2.11 and two longitudinal stiffeners elements. According to Wutzow and De Paiva (2008), stiffeners are typically linear elements with a negligible thickness. Stiffeners are treated as a line continuum in this study.

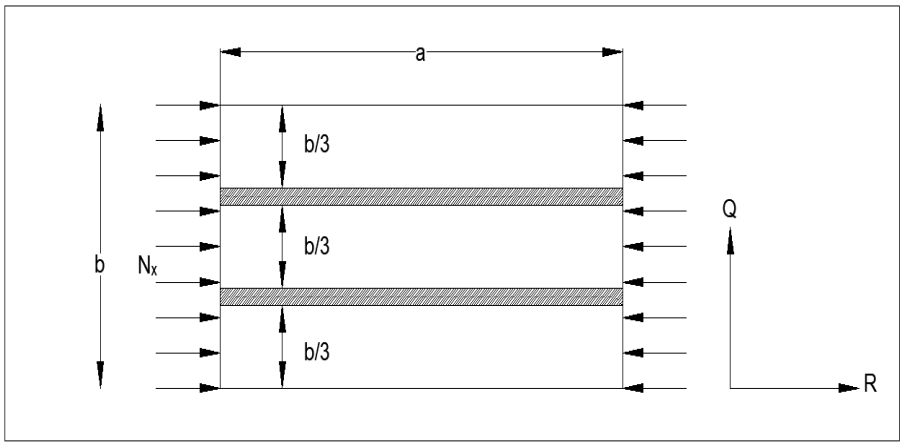

Figure 2.11: Stiffened System Under In-plane Load.

Ibeabuchi (2014) [7] derived the governing Equation for stiffened rectangular isotropic plates from the principles of elasticity theory as follows:

$$\begin{aligned}&\frac{1}{P^4}\frac{\partial^4 W}{\partial R^4}+\frac{2}{P^2}\cdot\frac{\partial^4 W}{\partial R^2\partial Q^2}+\frac{\partial^4 W}{\partial Q^4}+\frac{1}{P^4}\cdot\sum_{i=1}^{\infty}\gamma_i\left(\frac{\partial^4 w}{\partial R^4}\right)_{Q=C_i}\\&+\frac{b^2}{P^2}\cdot\frac{N_x}{D}\cdot\frac{\partial^2 W}{\partial R^2}+\frac{b^2}{P^2}\cdot\frac{N_x}{D}\cdot\sum_{i=1}^{\infty}\delta_i\left(\frac{\partial^2 W}{\partial R^2}\right)_{Q=C_i}=0\end{aligned}\tag{2.104}$$

where, Q and R are non dimensional parameter.

and $Q=\frac{y}{b}$ that is $y=bQ$; $R=\frac{x}{a}$ that is $x=aR$
$\gamma_i=\frac{EI_i}{Db}$ = Ratio of bending stiffness rigidity of stiffeners to the plate.
$\delta_i=\frac{A_i}{bh}$ = Ratio of cross-sectional area of the stiffeners to the plate.

The product of average force and distance traveled by the force is defined mathematically as work. As a result, Equation 2.104 becomes; for the combined action of work done on the stiffened system by the compressive and resistive forces over a distance w.

$$\begin{aligned}\Pi=\frac{1}{2}\Bigg[&\frac{A^2}{P^4}\cdot H\frac{\partial^4 H}{\partial R^4}+\frac{2A}{p^2}\cdot H\frac{\partial^4 H}{\partial R^2\partial Q^2}+A^2\frac{H\cdot\partial^4 H}{\partial Q^4}+\frac{A^2}{P^4}\cdot\sum_{i=1}^{\infty}\gamma_i\left(\frac{H\cdot\partial^4 H}{\partial R^4}\right)_{Q=C_i}\\&+\frac{b^2}{P^2}\cdot\frac{N_xA^2}{D}\frac{H.\partial^2 H}{\partial R^2}+\frac{b^2}{P^2}\cdot\frac{N_xA^2}{D}\sum_{i=1}^{n}\delta_i\left(\frac{H.\partial^2 H}{\partial R^2}\right)_{Q=C_i}=ei\end{aligned}\tag{2.105}$$

Where; Deflection function, $W=AH$; A = coefficient; H is the shape function: ei is the

introduced error, "i" is the number of points on the continuum.
Integrating Equation 2.105 twice with respect to R and Q gave;

(2.106)

$$\Pi = \frac{A^2}{2}\int_0^1\int_0^1\left[\frac{H}{P^4}\cdot\frac{\partial^4 H}{\partial R^4}+\frac{2H}{p^2}\cdot\frac{\partial^4 H}{\partial R^2\partial Q^2}+\frac{H\cdot\partial^4 H}{\partial Q^4}+\frac{1}{P^4}\cdot\sum_{i=1}^{\infty}\gamma_i\left(\frac{H\cdot\partial^4 H}{\partial R^4}\right)_{Q=C_i}\right]\partial R\partial Q$$
$$+\frac{A^2b^2}{2P^2}\cdot\frac{N_x}{D}\int_0^1\int_0^1\left[\frac{H.\partial^2 H}{\partial R^2}+\sum_{i=1}^{n}\delta_i\left(\frac{H.\partial^2 H}{\partial R^2}\right)_{Q=C_i}\right]\partial R\partial Q$$

Π is the Total Work error Functional. Minimizing and making N_x the subject of Equation 2.4.2 gave;

$$N_{x(critical)} = \frac{D\int_0^1\int_0^1\left[\frac{H}{P^2}\cdot\frac{\partial^4 H}{\partial R^4}+2H\cdot\frac{\partial^4 H}{\partial R^2\partial Q^2}+P^2\frac{H\cdot\partial^4 H}{\partial Q^4}+\frac{1}{P^2}\cdot\sum_1^n\gamma_i\left(\frac{H\cdot\partial^4 H}{\partial R^4}\right)_{Q=c_i}\right]\partial R\partial Q}{-b^2\int_0^1\int_0^1\left[\frac{H.\partial^2 H}{\partial R^2}+\sum_1^n\delta_i\left(\frac{H.\partial^2 H}{\partial R^2}\right)_{Q=c_i}\right]\partial R\partial Q} \tag{2.107}$$

Equation 2.107 is the Buckling equation for rectangular plate stiffened longitudinally under in-plane loading.

2.4.3 Boundary Conditions for SSSS Stiffened Plates.

Now, Figure 2.12 depicts a stiffened plate with simply supported edges and dimensionless R-Q axes. In a dimensionless coordinate system, the boundary conditions are as follows:

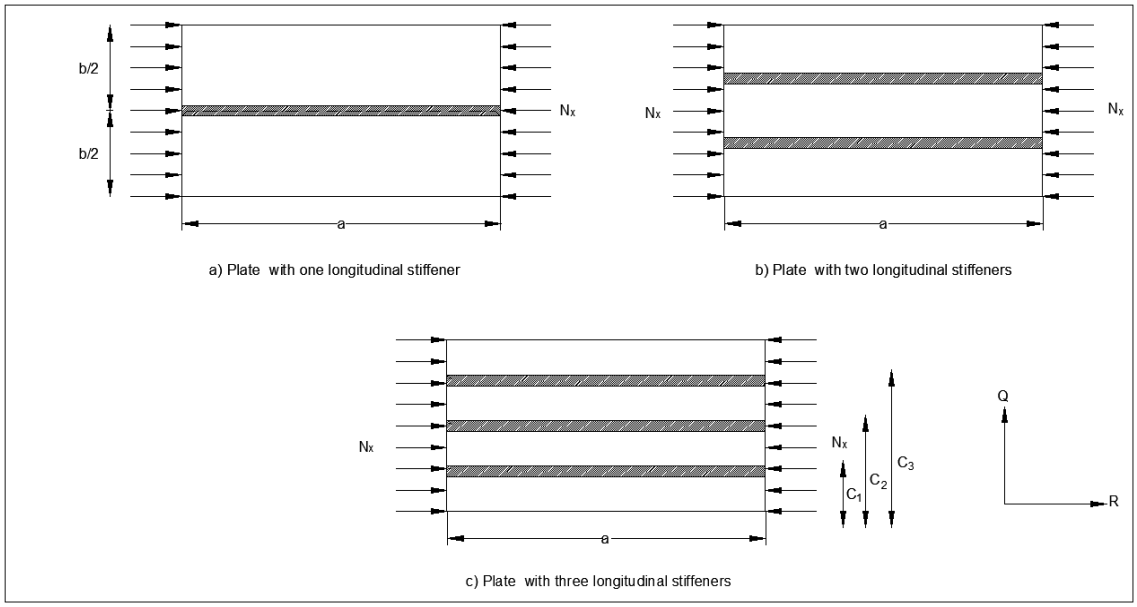

Figure 2.12: Stiffeners Arrangement for SSSS Stiffened Plates

$$w(R=0)=\frac{\partial^2 w}{\partial R^2}(R=0)=0; w(R=1)=\frac{\partial^2 w}{\partial R^2}(R=1)=0$$
$$w(Q=0)=\frac{\partial^2 w}{\partial Q^2}(Q=0)=0; w(Q=1)=\frac{\partial^2 w}{\partial^2 Q}(Q=1)=0$$

After deriving the formula the value of buckling load can be obtained as follows:
Case of One Stiffener:

$$N_x=\frac{\pi^2 D}{b^2 P^2}\frac{\left[\left(1+P^2\right)^2+1.997\gamma\right]}{[1+1.985\delta]}$$

Where,

$$K=\frac{\left[\left(1+P^2\right)^2+1.997\gamma\right]}{[1+1.985\delta]}$$

Stiffeners Case of Two:

$$N_x=\frac{\pi^2 D}{b^2 P^2}\frac{\left[\left(1+P^2\right)^2+3\gamma\right]}{[1+2.9630\delta]}$$

Where,

$$K=\frac{\left[\left(1+P^2\right)^2+3\gamma\right]}{[1+2.9630\delta]}$$

Stiffeners Case of Three:

$$N_x=\frac{\pi^2 D}{b^2 P^2}\frac{\left[\left(1+P^2\right)^2+4.0048\gamma\right]}{[1+3.8445\delta]}$$

Where,

$$K = \frac{\left[\left(1+P^2\right)^2 + 4.0048\gamma\right]}{[1+3.8445\delta]}$$

Timoshenko and Gere (1961) used the Energy Principle in the Ritz method to calculate buckling coefficients for the following three cases: K was calculated for the cases of one, two, and three longitudinal stiffeners. where the corresponding buckling coefficient are as follows:

$$K = \frac{\left(1+\beta^2\right)^2 + 2\gamma}{\beta^2(1+2\delta)}; K = \frac{\left(1+\beta^2 2+3y\right)}{\beta^2(1+3\delta)}; K = \frac{\left(1+\beta^2\right)^2 + 4\gamma}{\beta^2(1+4\delta)} \tag{2.108}$$

Where; β represents aspect ratio, γ represents the ratio of flexural rigidity of stiffener to that of plate, δ represents the cross-sectional area of stiffener to that of plate.

CHAPTER 3

MODELLING

3.1 Modelling of Plate

For modelling the plate, SHELL 281 element has been used to model the geometry of isotropic thin plate whose element property has been described in the previous section. The geometric dimensions of the thin plate used for the research work is presented in Table 3.1. The Geometry has been modelled in the Design Modeller of ANSYS.

Length (mm)	Width (mm)	Thickness(mm)
2000	1000	10

Table 3.1: Geometry dimensions of the plate

Four isotropic materials that are used for this study are as follows:

- Mild Steel
- AISI 1090 Steel
- Stainless Steel 302
- Stainless Steel 330

The isotropic properties of the materials as obtained from[9] are tabulated in Table 3.2.

Material	Mild Steel	AISI 1090 Steel	Stainless Steel 302	Stainless Steel 330
E (GPa)	200	205	193	197
N	0.3	0.29	0.25	0.27
Density (Kg/m^3)	7850	7850	7860	8000

Table 3.2: Mechanical properties of the isotropic materials.

3.2 Mesh Element

Quadrilateral Meshing has been used to mesh the plates and the stiffened plates. In *ANSYS*, the global Element Order option allows us to control whether meshes are to be created with midside nodes (quadratic elements) or without midside nodes (linear elements) where the element types are shown in Figure 3.1. Reducing the number of midside nodes reduces the number of degrees of freedom. Choices for the global Element Order option include Program Controlled, Linear, and Quadratic. The Quadratic option retains midside nodes on elements created in the part or body. All elements will have midside nodes. If Element Order is set to Quadratic, and if Straight Sided Elements is set to No, the midside nodes will be placed on the geometry so that the mesh elements properly capture the shape of the geometry. However, if the location of a midside node might affect the mesh quality, the midside node may be relaxed to improve the element shape. Therefore, some midside nodes might not follow the shape of the geometry precisely.

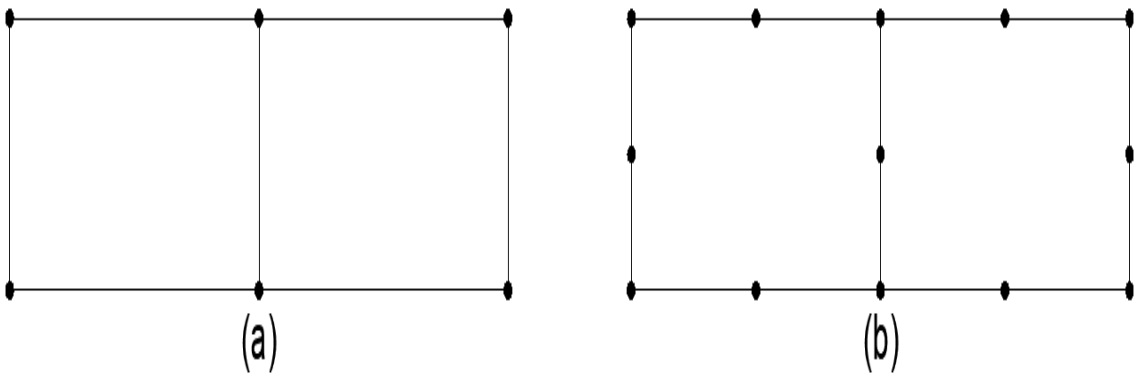

Figure 3.1: (a) Linear and (b) Quadratic Element

3.3 Boundary Condition

The boundary condition has the greatest impact on the buckling load of any engineering structure subjected to uniformly compressive in-plane load. In ANSYS, a plate can be modelled as a shell model or solid model. In this study, both the plates and the stiffeners have been modelled as shell elements.For shell models, the boundary conditions used for this work are stated as follows:

Shell models are based on the Shell181 or Shell281 shell elements. A plate shell model is a large region divided into smaller shell parts. At their nodes, shell elements have degrees of freedom for translation (UX, UY, and UZ) and rotation (ROTX, ROTY, and ROTZ). Two essential points regarding the effects of boundary conditions on those degrees of freedom

must be noted. To begin, edge rotation in the thickness direction (UZ) is actually inplane displacements (UX and UY). As a result, restraining ROTZ also means restraining inplane displacements. To look at it another way, if inplane displacements (UX and UY) are allowed, ROTZ must be allowed as well. Secondly, out-of-plane displacement is defined as rotation of an edge about an inplane axis perpendicular to the edge.[5] The boundary conditions for shell model of a plate are shown in the Figure 3.2.

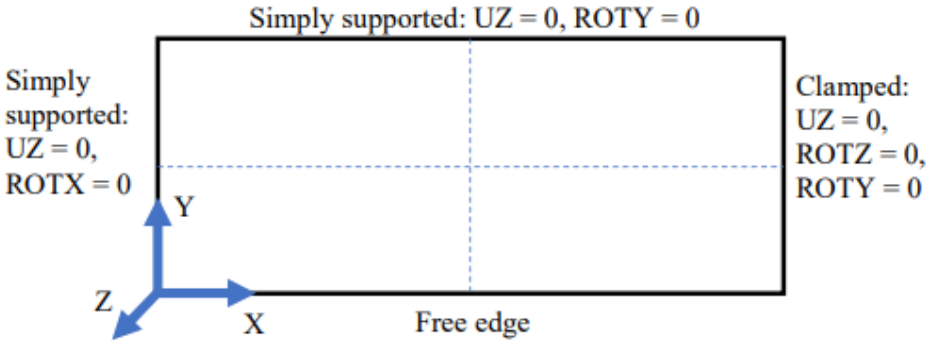

Figure 3.2: Boundary Conditions on shell model of plate

3.4 Additional consideration for boundary conditions in ANSYS

Despite the fact that the plate is under balanced forces, the model may require additional boundary conditions to restrain rigid body translation and rotation. For instance, in the case of a full plate model with all edges simply supported, additional constraints must be added to prevent body movement that is rigid. In general, the constraining of two distinct points on the plate should be avoided sufficient to prevent rigid body movement under any loading/boundary conditions configuration.This has been illustrated in Figure 3.3

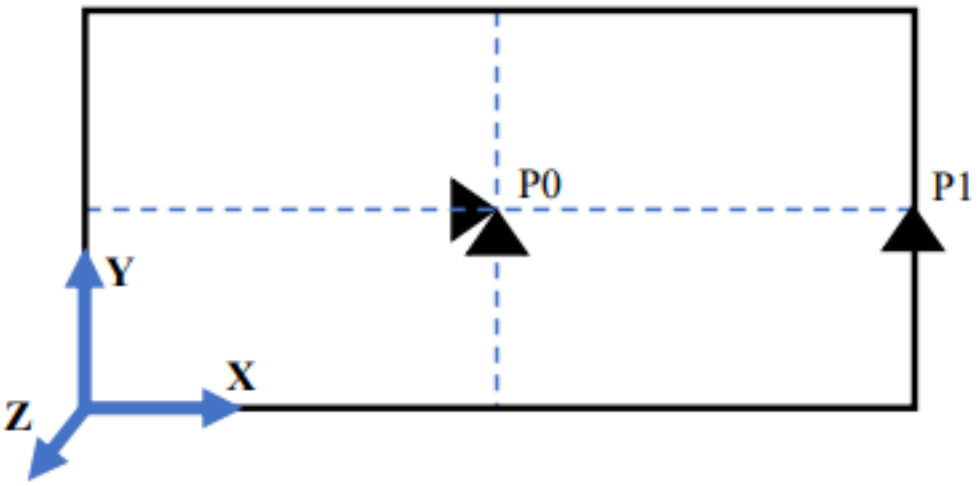

Figure 3.3: Additional Boundary conditions for full shell model of plate

3.5 Modelling of Stiffened Plates

A stiffened plate is a combination of one or more stiffeners attached to a plate. All the stiffened plates chosen here have the same element type as that of the plate. The cross section of a stiffened plate is illustrated in Figure 3.4 and the dimensions of the stiffeners as mentioned in [9] are mentioned in Table 3.3

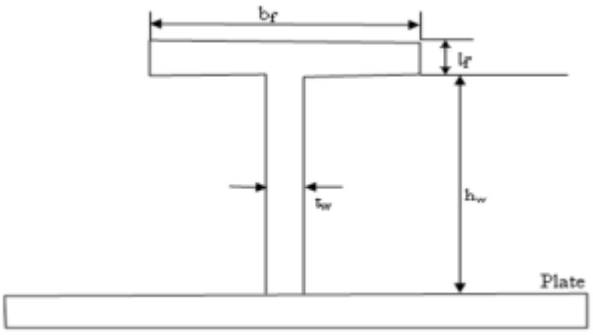

Figure 3.4: Cross Section of Stiffened Plate

Cross Section of Stiffener (mm)	t_w	h_w	t_f	b_f
Rectangular Shape	8	35	-	-
L-shape	7.5	35	4	20
T-shape	7.5	35	6	26

Table 3.3: Dimension of the stiffeners

To make the attachment between stiffener and plate CONTA 174 and TARGET 170 and to keep the bonded contact together. ANSYS itself provides the multipoint constraint (MPC) algorithm.

The contact between the plate and the stiffener is an important criteria in obtaining the solution results in the finite element analysis software ANSYS. For a rectangular plate, the target surface is the face of the plate and the contact surface is the edge of the stiffener or the edges of the stiffener depending on its number.This has been illustrated in Figure 3.5. For an L-shaped plate, there are two contacts. On the first contact, the target surface is the plate surface and contact surface is one edge of the L stiffener. For the second target surface, the face of the flange is selected and 3 edges have been selected as the contacts.This has been illustrated in Figure 3.6. For a T shaped stiffened plate, there are two contacts as well. The first contact has a target surface assigned as the plate face and the contact surface as one edge in contact or more than one edge in contact in case of multiple stiffeners. The second contact has one target surface as the face of the flange or more faces in case of multiple stiffeners and two edges as contact surface or multiple of two edges in case of more than one stiffeners.This has been illustrated in Figure 3.7.

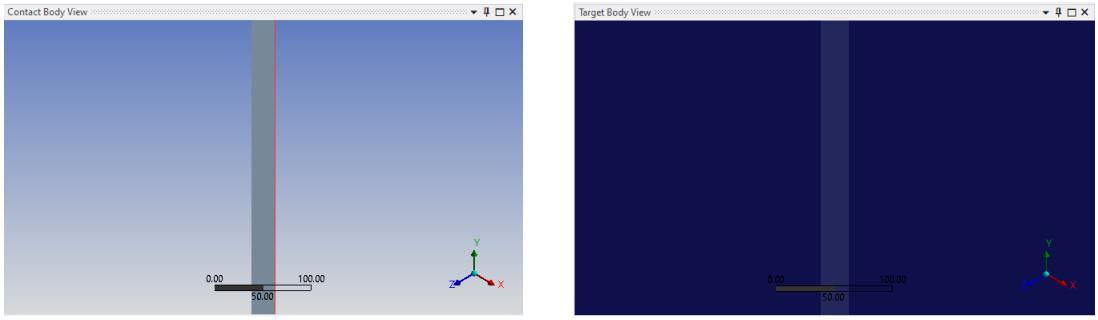

Figure 3.5: Contact and Target Surfaces for rectangular shaped stiffened plate

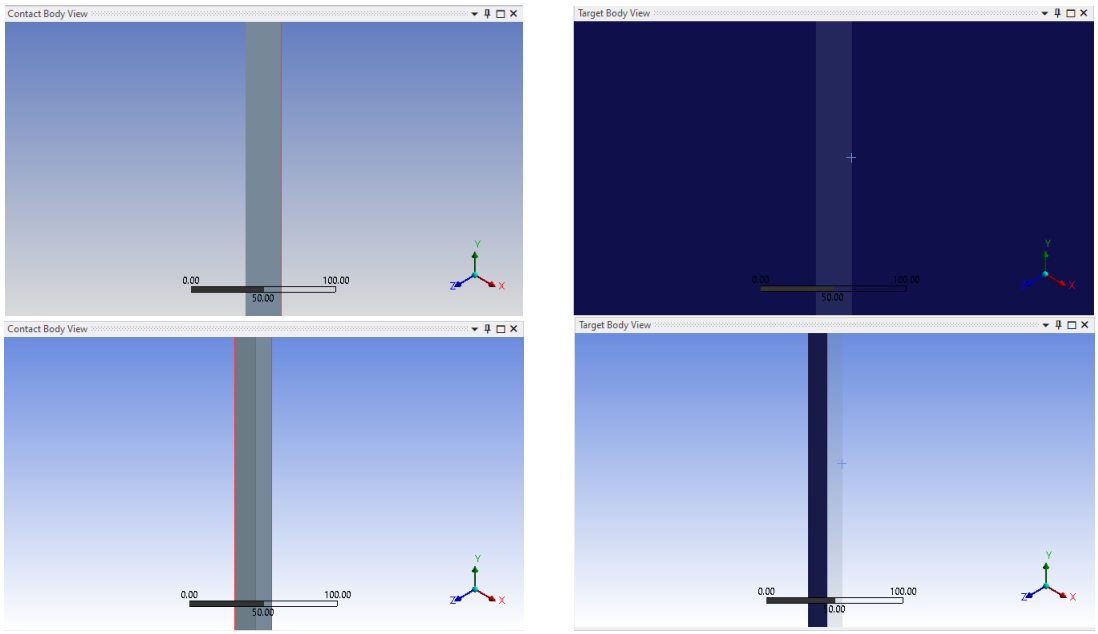

Figure 3.6: Contact and Target Surfaces for L-shaped stiffened plate

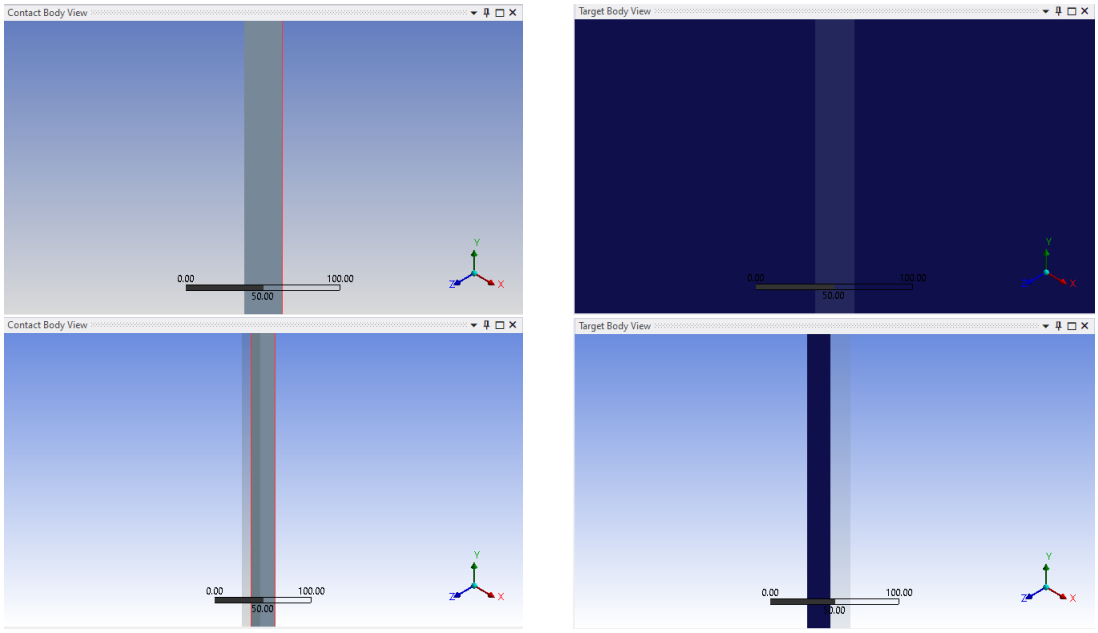

Figure 3.7: Contact and Target Surfaces for T-shaped stiffened plate

CHAPTER 4

VALIDATION AND RESULTS

4.1 Linear Buckling Analysis of a Simply Supported (SSSS) Plate:

4.1.1 Mesh Convergence Study

In the first step of the analysis, the mesh convergence study is done for the isotropic plates and solutions are found theoretically and via simulation for the simply supported boundary condition on all edges of the plate. The process of mesh convergence involves decreasing the element size and analysing the impact of this process on the accuracy of the solution. Typically, the smaller the mesh size, the more accurate the solution as the behaviour of the design or product is better sampled across its physical domain. The higher the accuracy, the larger the simulations can become in terms of data to store and handle, which translates to longer runtimes. Mesh convergence is done to maintain a balance between accuracy and runtime.The purpose of mesh convergence study is to optimise the mesh element size and number of mesh element.

Figure 4.1 represents the number of mesh elements taken for accurate results. Here, an AISI steel plate has been taken initially and analysed to check the meshing, boundary condition and loading condition to find the critical load.Here the load applied along the in-plane is 1 N/mm which when multiplied with the load multiplier 1 will provide the critical buckling load.The critical load obtained from the theoretical solution and that of the analysis are compared with an increasing number of mesh elements to converge the results to a minimum error percentage. The result is thus validated for a specific number of mesh elements and beyond that number, the results would practically obtain the same result but will take more time for the simulation to occur. So, the optimised number of elements is 5000 where the size of each element is 20 mm. This is checked for all the other three elements.A graph has been plotted between critical load versus number of mesh elements as shown in Figure 4.2 From the graph, it is seen that the material AISI 1090 Steel yields the highest

critical load as its bending stiffness is higher compared to the other materials.

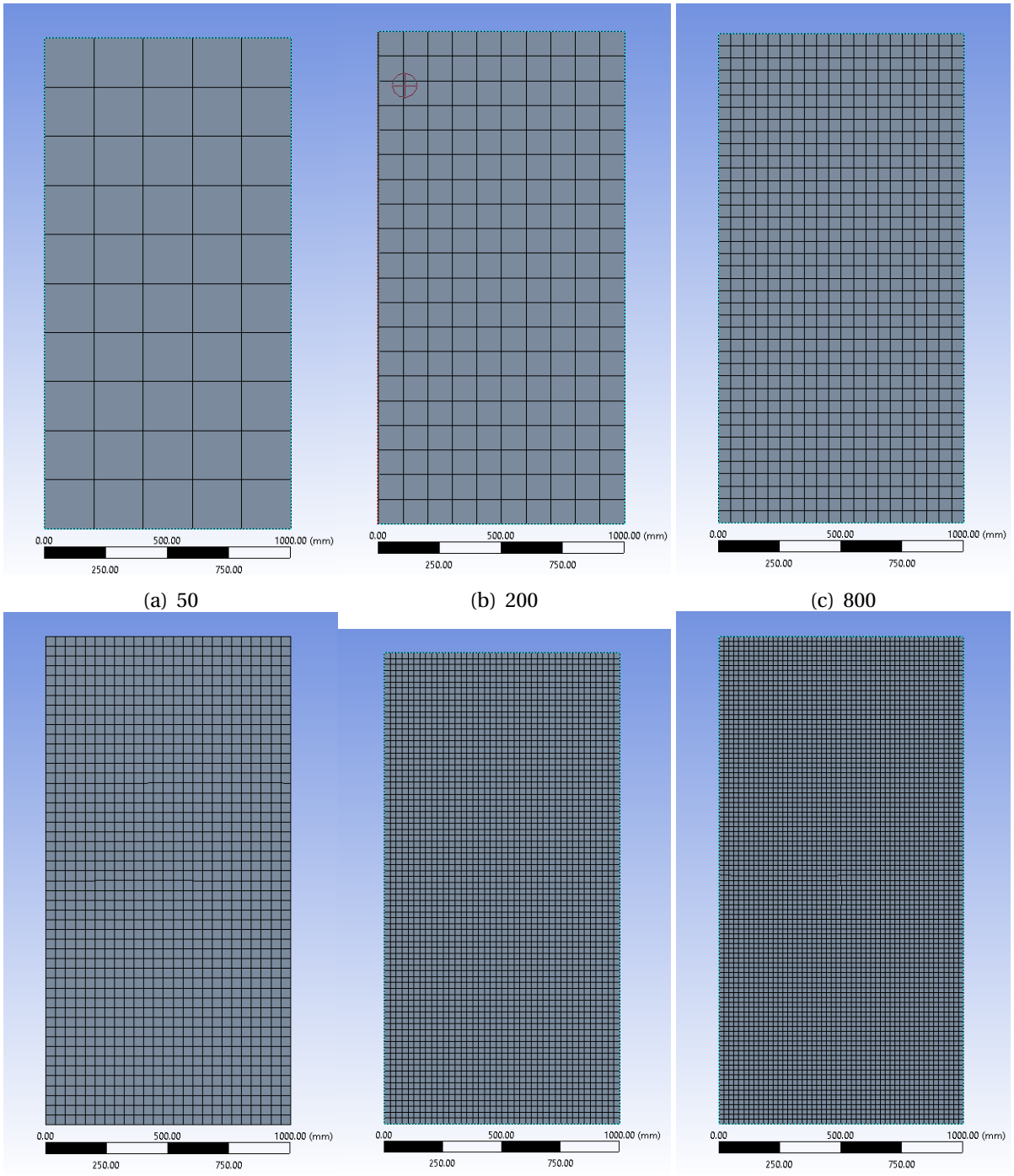

(a) 50 (b) 200 (c) 800

(d) 1250 (e) 3200 (f) 5000

Figure 4.1: Number of mesh refinement elements

AISI 1090 Steel				
Number of Mesh Element	Load Multiplier	Critical Buckling Load (Present Study) (N/mm)	Theoretical Critical Buckling Load (N/mm)	Percent Difference with Theoretical Value
50	1	774.36	736.3534	5.1615
200	1	746.21	736.3534	1.3386
800	1	738.49	736.3534	0.2902
1250	1	737.44	736.3534	0.1476
3200	1	736.58	736.3534	0.0308
5000	1	736.35	736.3534	0.0005

Table 4.1: Mesh convergence and validation of result of AISI 1090 Steel

Mild Steel				
Number of Mesh Element	Load Multiplier	Critical Buckling Load (Present Study) (N/mm)	Theoretical Critical Buckling Load (N/mm)	Percent Difference with Theoretical Value
50	1	760.13	723.0513	5.1281
200	1	732.71	723.0513	1.3358
800	1	725.14	723.0513	0.2889
1250	1	724.24	723.0513	0.1644
3200	1	723.26	723.0513	0.0289
5000	1	723.04	723.0513	0.0016

Table 4.2: Mesh convergence and validation of result of Mild Steel

Stainless Steel 302				
Number of Mesh Element	Load Multiplier	Critical Buckling Load (Present Study) (N/mm)	Theoretical Critical Buckling Load (N/mm)	Percent Difference with Theoretical Value
50	1	713.12	677.2774	5.2922
200	1	686.42	677.2774	1.3499
800	1	679.27	677.2774	0.2942
1250	1	678.32	677.2774	0.1539
3200	1	677.51	677.2774	0.0344
5000	1	677.29	677.2774	0.0019

Table 4.3: Mesh convergence and validation of result of Stainless Steel 302

Stainless Steel 330				
Number of Mesh Element	Load Multiplier	Critical Buckling Load (Present Study) (N/mm)	Theoretical Critical Buckling Load (N/mm)	Percent Difference with Theoretical Value
50	1	735.61	699.0692	5.2271
200	1	708.47	699.0692	1.3448
800	1	701.11	699.0692	0.2919
1250	1	700.12	699.0692	0.1503
3200	1	699.29	699.0692	0.0316
5000	1	699.07	699.0692	0.0001

Table 4.4: Mesh convergence and validation of result of Stainless Steel 330

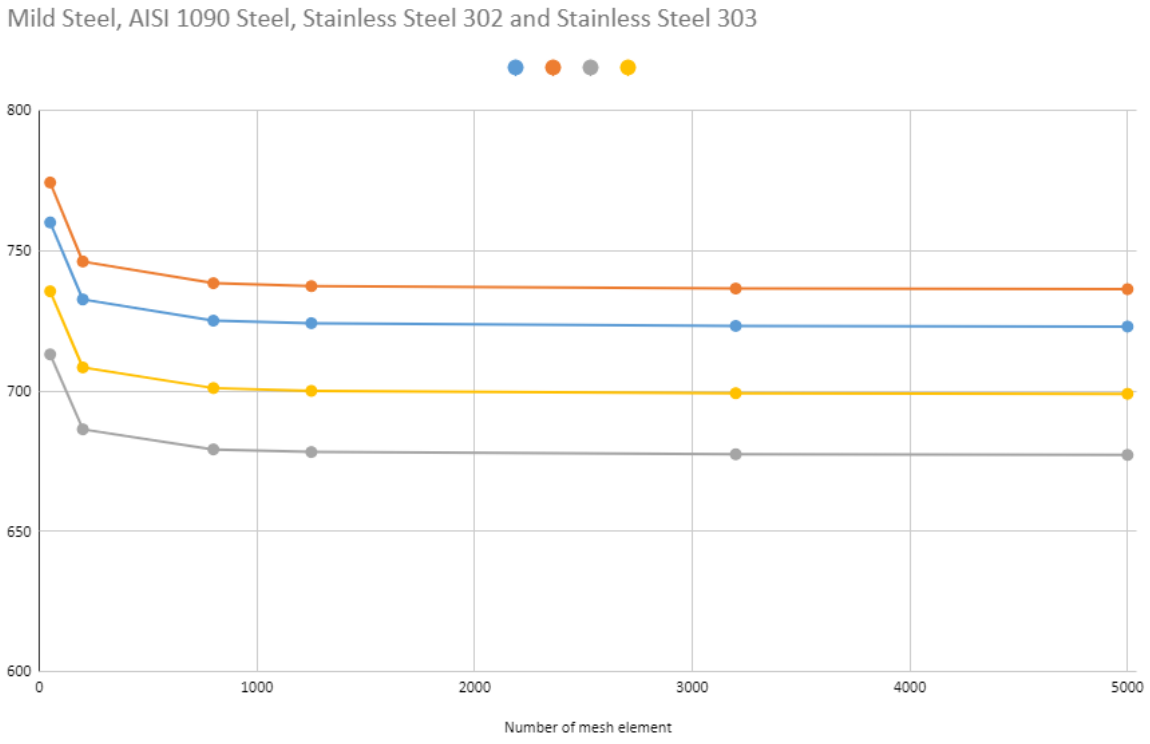

Figure 4.2: Critical Buckling Load vs Number of Mesh Elements

4.1.2 Simulation Results of a Simply Supported (SSSS) Rectangular Plate in ANSYS

The results of the simulations for a rectangular plate simply supported on all sides are shown below in Figure 4.3 and Figure 4.4

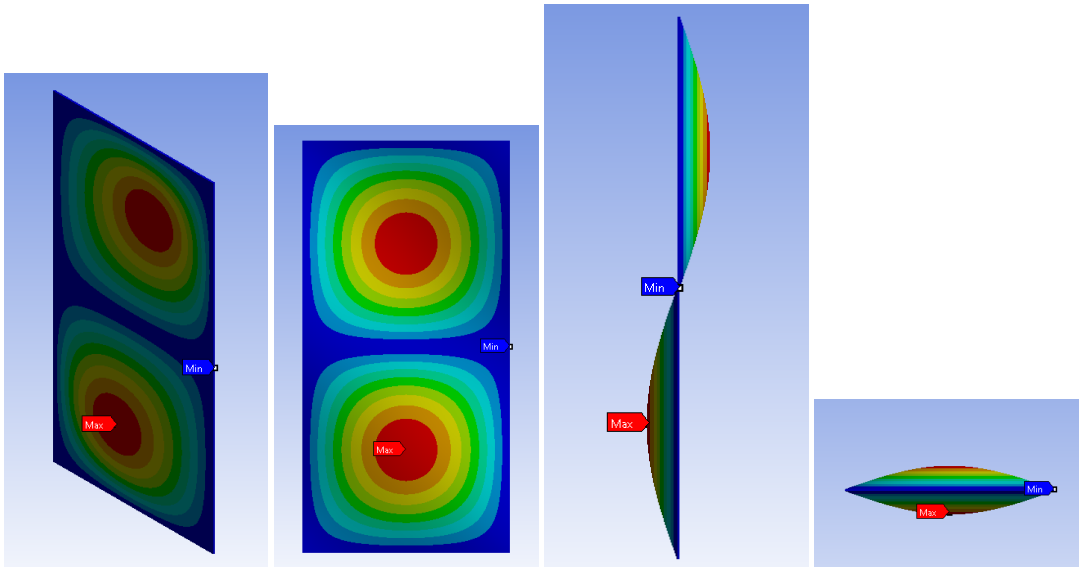

(a) Isometric View (b) Front view (c) Side View (d) Top View

Figure 4.3: Mode 1 (2,1) result of a simply supported plate (AISI 1090 Steel); N_{cr}= 736.35 N/mm)

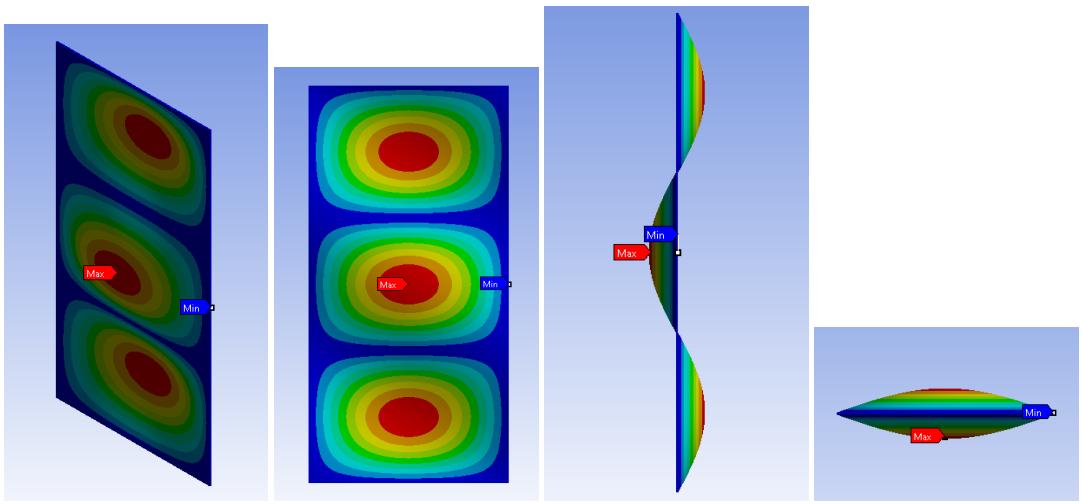

(a) Isometric View (b) Front view (c) Side View (d) Top View

Figure 4.4: Mode 2 (3,1) result of result of a simply supported plate (AISI 1090 Steel); N_{cr}= 864.23 N/mm)

4.2 Linear Buckling Analysis of a Clamped (CCCC) Plate:

The theoretical critical buckling loads for linear buckling for the four types of materials have been calculated from the chart in Figure 2.9 to calculate the value of K_c for the loaded edges clamped as illustrated by a mark in the following Figure 4.5.The value of K_c thus obtained for the four plates is 7.9. The theoretical Critical Buckling Load is calculated and then the deviations are found out from the simulation values. The error percentages in all the cases are significantly low, less than 0.5 percent.A bar chart showing the deviations in the two values is shown in Figure 4.6

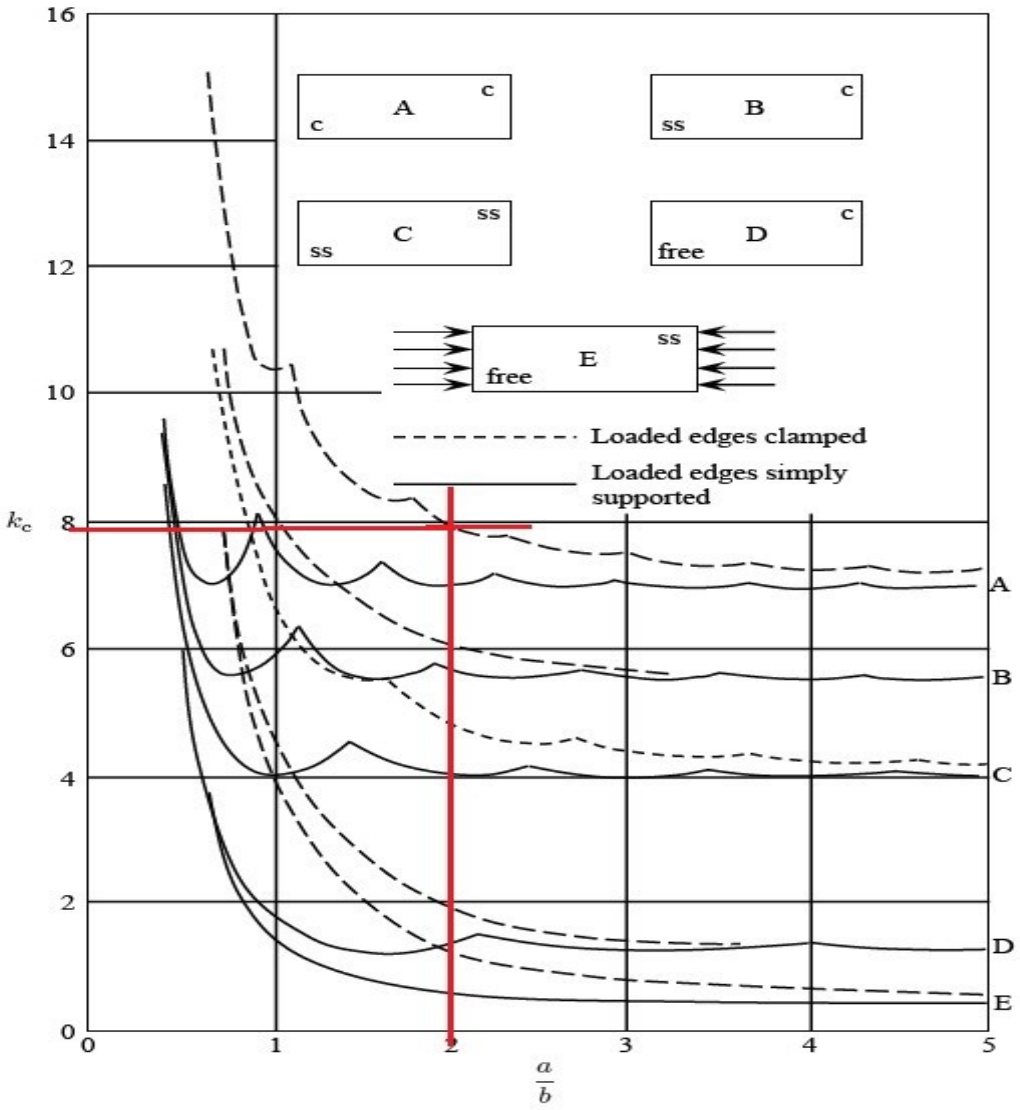

Figure 4.5: Buckling Coefficient of a Clamped Rectangular Plate

For Rectangular Clamped Plate				
Material Type	Kc	Theoretical Critical Buckling Load (N/mm)	Buckling Load Obtained from Simulation	Deviation Percentage
Mild Steel	7.9	1428.03	1421.6	0.45
AISI 1090 Steel	7.9	1454.3	1448.7	0.39
Stainless Steel 302	7.9	1337.62	1331.8	0.44
Stainless Steel 330	7.9	1380.66	1374.5	0.45

Table 4.5: Critical buckling load of a rectangular clamped plate

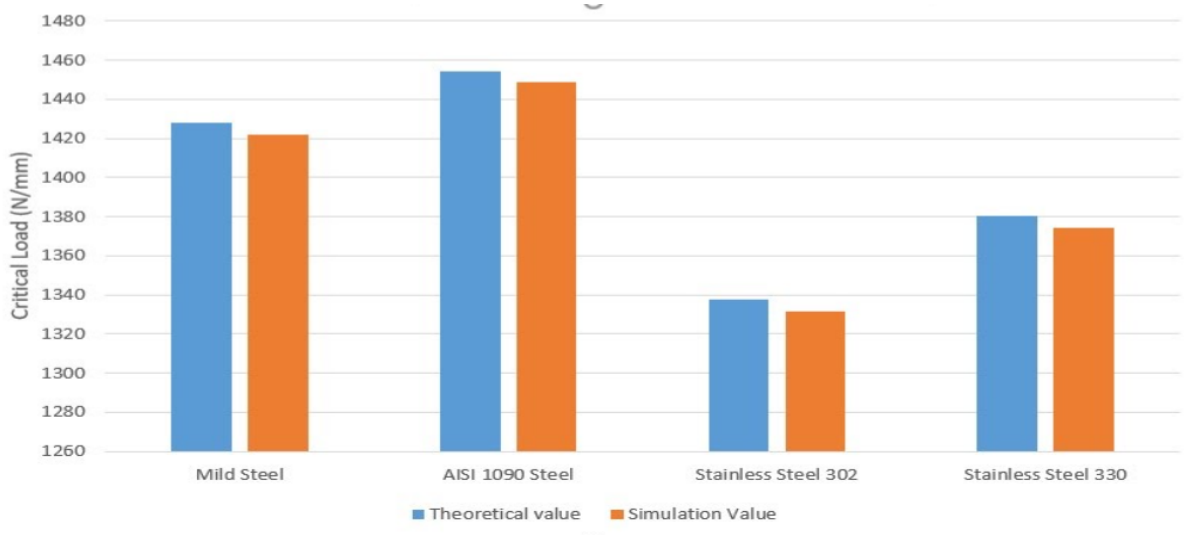

Figure 4.6: Deviations of Theoretical and Simulation values of a Clamped Plate

4.2.1 Simulation Results of a Clamped (CCCC) Rectangular Plate in ANSYS

The results of the simulations for a rectangular plate clamp supported on all sides are shown below in Figure 4.7 and Figure 4.8

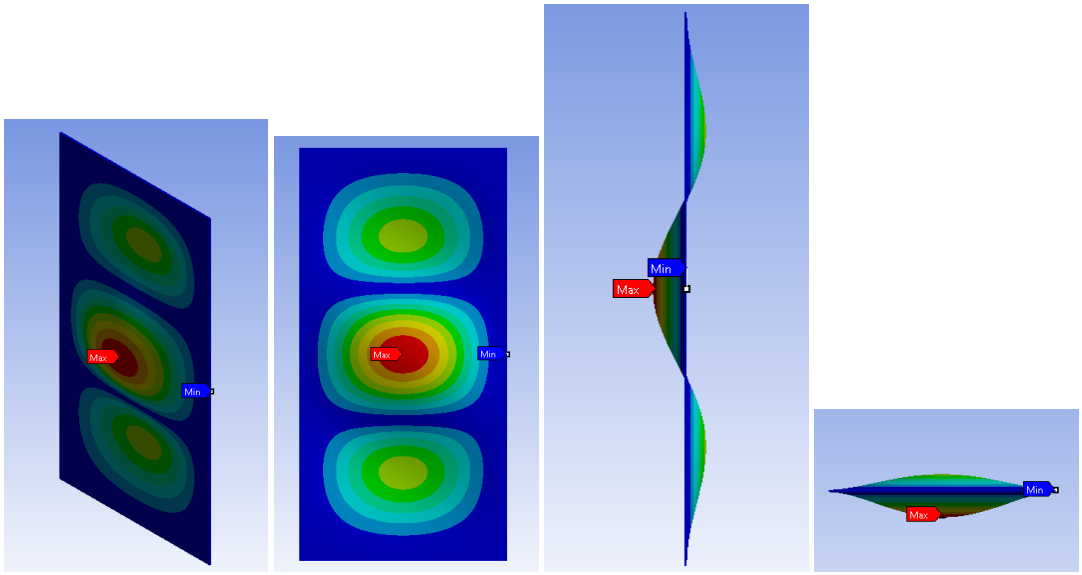

(a) Isometric View (b) Front view (c) Side View (d) Top View

Figure 4.7: Mode 1 (3,1) result of a clamped plate (AISI 1090 Steel); N_{cr}= 1447.8 N/mm)

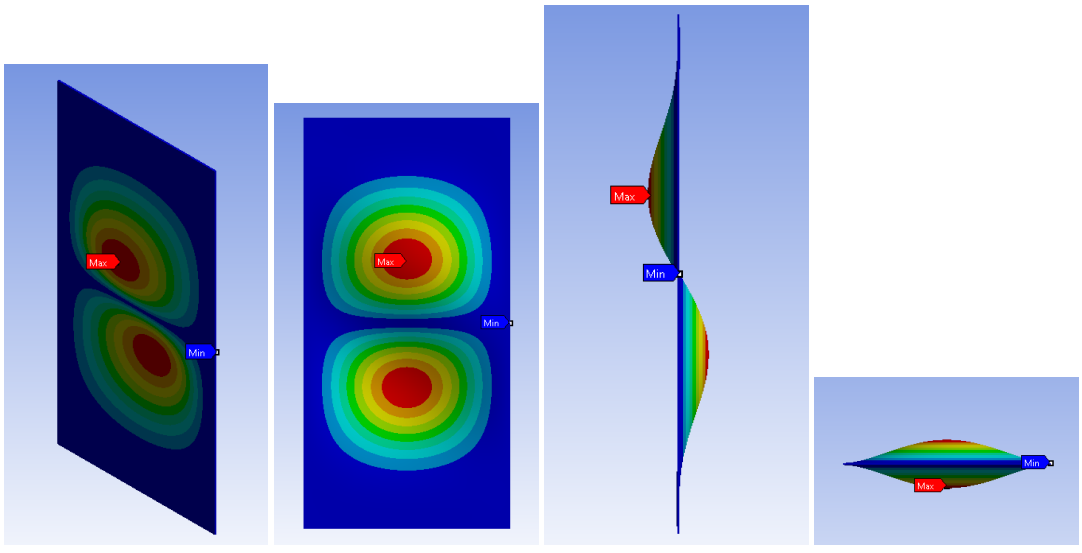

(a) Isometric View (b) Front view (c) Side View (d) Top View

Figure 4.8: Mode 1 (2,1) result of result of a clamped plate (AISI 1090 Steel); N_{cr}= 1488.38 N/mm)

4.3 Linear Buckling Analysis of a Simply Supported (SSSS) Stiffened Plate

4.3.1 One Box Shaped Stiffener

The dimensions of the plate and the box shaped stiffener attached to the plate are taken from Table 3.1 and Table 3.3. The stiffener is attached in the middle of the plate along its length. The calculation of theoretical results as obtained from the formulation in [7] are shown in the following table:

Plate Specification	
Length	2 m
Breadth	1 m
Thickness	0.01 m
Aspect Ratio (P)	2
AISI 1090 Steel	
Moment of Inertia (I)	0.0000001143333333 m^4
Flexural Stiffness (D)	18651.96
Sectional Area	0.00028 m^2
Ratio of Bending Stiffness Rigidity of Stiffeners to the Plate (γ)	1.2566
Ratio of Cross Sectional Areas of the Stiffeners to the Plate (δ)	0.028
Buckling Coefficient (K)	6.512
Critical Load (Theoretical)	1198.808 N/mm
Critical Load (Simulation)	1222.2 N/mm
Error Percentage	1.95%

Table 4.6: Theoretical Result of a rectangular plate with one box stiffener attached (AISI 1090 Steel)

Plate Specification	
Length	2 m
Breadth	1 m
Thickness	0.01 m
Aspect Ratio (P)	2
Mild Steel	
Moment of Inertia (I)	0.0000001143333333 m^4
Flexural Stiffness (D)	18315.02
Sectional Area	0.00028 m^2
Ratio of Bending Stiffness Rigidity of Stiffeners to the Plate (γ)	1.2485
Ratio of Cross Sectional Areas of the Stiffeners to the Plate (δ)	0.028
Buckling Coefficient (K)	6.51
Critical Load (Theoretical)	1177.15 N/mm
Critical Load (Simulation)	1199.2 N/mm
Error Percentage	1.87%

Table 4.7: Theoretical Result of a rectangular plate with one box stiffener attached (Mild Steel)

Plate Specification	
Length	2 m
Breadth	1 m
Thickness	0.01 m
Aspect Ratio (P)	2
Stainless Steel 302	
Moment of Inertia (I)	0.0000001143333333 m^4
Flexural Stiffness (D)	17155.56
Sectional Area	0.00028 m^2
Ratio of Bending Stiffness Rigidity of Stiffeners to the Plate (γ)	1.2862
Ratio of Cross Sectional Areas of the Stiffeners to the Plate (δ)	0.028
Buckling Coefficient (K)	6.526
Critical Load (Theoretical)	1104.99 N/mm
Critical Load (Simulation)	1127.6 N/mm
Error Percentage	2.05%

Table 4.8: Theoretical Result of a rectangular plate with one box stiffener attached (Stainless Steel 302)

Plate Specification	
Length	2 m
Breadth	1 m
Thickness	0.01 m
Aspect Ratio (P)	2
Stainless Steel 330	
Moment of Inertia (I)	0.0000001143333333 m^4
Flexural Stiffness (D)	17707.55
Sectional Area	0.00028 m^2
Ratio of Bending Stiffness Rigidity of Stiffeners to the Plate (γ)	1.2720
Ratio of Cross Sectional Areas of the Stiffeners to the Plate (δ)	0.028
Buckling Coefficient (K)	6.519
Critical Load (Theoretical)	1139.37 N/mm
Critical Load (Simulation)	1162.1 N/mm
Error Percentage	1.99%

Table 4.9: Theoretical Result of a rectangular plate with one box stiffener attached (Stainless Steel 330)

4.3.1.1 Simulation Results for One Box Shaped Stiffener

The simulation results for one box shaped stiffener attached plate are shown below. The mode shape patterns are the same for different materials with varying critical load. The first and second mode shapes are shown as follows in Figure 4.9 and in Figure 4.10

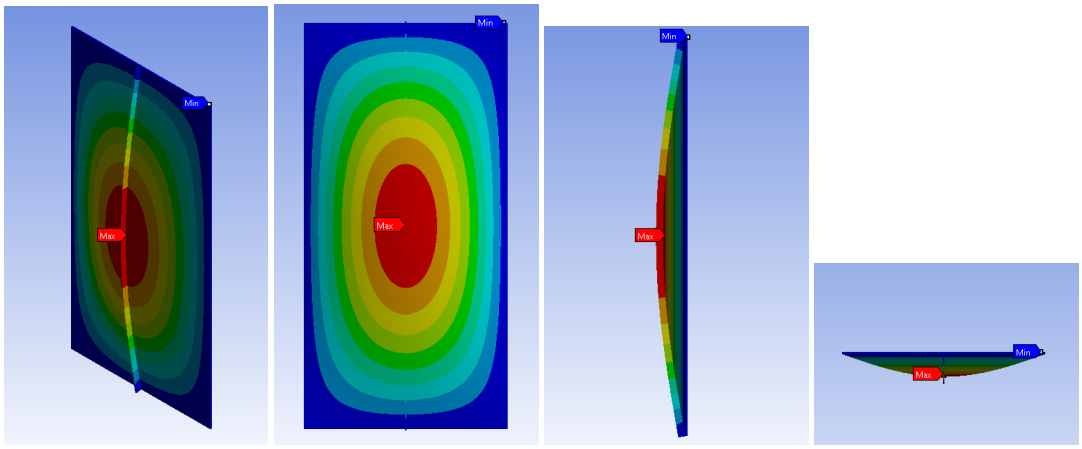

(a) Isometric View (b) Front view (c) Side View (d) Top View

Figure 4.9: Mode 1 (1,1) result of a box shaped stiffened plate (AISI 1090 Steel); N_{cr}= 1222.2 N/mm)

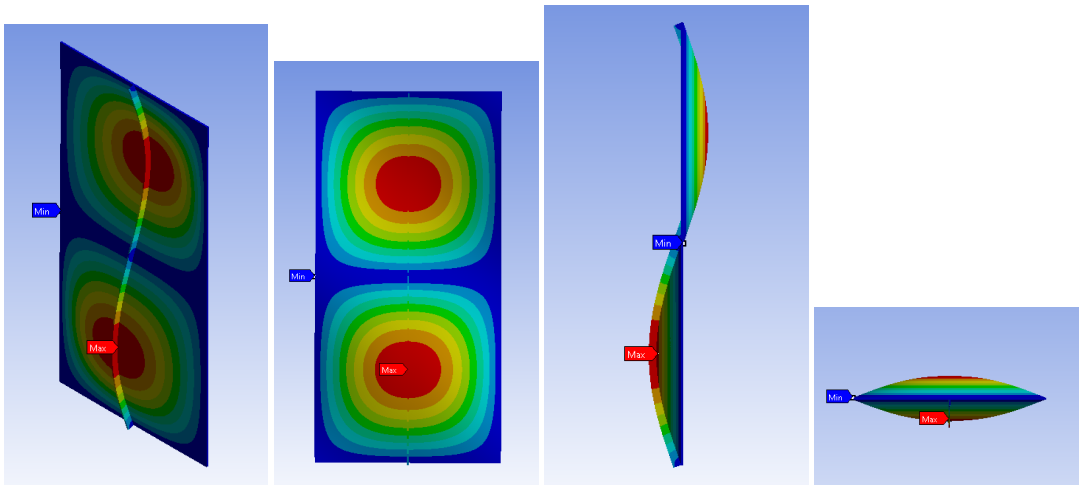

(a) Isometric View (b) Front view (c) Side View (d) Top View

Figure 4.10: Mode 2 (2,1) result of a box shaped stiffened plate (AISI 1090 Steel); N_{cr}= 1199.4 N/mm)

4.3.2 Three Box Shaped Stiffeners

The calculation of theoretical results as obtained from the formulation in [7] are shown in the following table:

Plate Specification	
Length	2 m
Breadth	1 m
Thickness	0.01 m
Aspect Ratio (P)	2
AISI 1090 Steel	
Moment of Inertia (I)	0.0000001143333333 m^4
Flexural Stiffness (D)	18651.96
Sectional Area	0.00028 m^2
Ratio of Bending Stiffness Rigidity of Stiffeners to the Plate (γ)	1.2566
Ratio of Cross Sectional Areas of the Stiffeners to the Plate (δ)	0.028
Buckling Coefficient (K)	6.778
Critical Load (Theoretical)	1247.83 N/mm
Critical Load (Simulation)	1290.1 N/mm
Error Percentage	3.38%

Table 4.10: Theoretical Result of a rectangular plate with three box stiffener attached (AISI 1090 Steel)

Plate Specification	
Length	2 m
Breadth	1 m
Thickness	0.01 m
Aspect Ratio (P)	2
Mild Steel	
Moment of Inertia (I)	0.0000001143333333 m^4
Flexural Stiffness (D)	18315.02
Sectional Area	0.00028 m^2
Ratio of Bending Stiffness Rigidity of Stiffeners to the Plate (γ)	1.2485
Ratio of Cross Sectional Areas of the Stiffeners to the Plate (δ)	0.028
Buckling Coefficient (K)	6.771
Critical Load (Theoretical)	1223.97 N/mm
Critical Load (Simulation)	1264.9 N/mm
Error Percentage	3.34%

Table 4.11: Theoretical Result of a rectangular plate with three box stiffener attached (Mild Steel)

Plate Specification	
Length	2 m
Breadth	1 m
Thickness	0.01 m
Aspect Ratio (P)	2
Stainless Steel 302	
Moment of Inertia (I)	0.0000001143333333 m^4
Flexural Stiffness (D)	17155.56
Sectional Area	0.00028 m^2
Ratio of Bending Stiffness Rigidity of Stiffeners to the Plate (γ)	1.2862
Ratio of Cross Sectional Areas of the Stiffeners to the Plate (δ)	0.028
Buckling Coefficient (K)	6.805
Critical Load (Theoretical)	1152.26 N/mm
Critical Load (Simulation)	1193.3 N/mm
Error Percentage	3.56%

Table 4.12: Theoretical Result of a rectangular plate with three box stiffener attached (Stainless Steel 302)

Plate Specification	
Length	2 m
Breadth	1 m
Thickness	0.01 m
Aspect Ratio (P)	2
Stainless Steel 330	
Moment of Inertia (I)	0.0000001143333333 m^4
Flexural Stiffness (D)	17707.55
Sectional Area	0.00028 m^2
Ratio of Bending Stiffness Rigidity of Stiffeners to the Plate (γ)	1.2720
Ratio of Cross Sectional Areas of the Stiffeners to the Plate (δ)	0.028
Buckling Coefficient (K)	6.79
Critical Load (Theoretical)	1187.08 N/mm
Critical Load (Simulation)	1228.3 N/mm
Error Percentage	3.47%

Table 4.13: Theoretical Result of a rectangular plate with three box stiffener attached (Stainless Steel 330)

4.3.2.1 Simulation Results for Three Box Shaped Stiffeners

The simulation results for three box shaped stiffeners attached plate are shown as follows in Figure 4.11 and in Figure 4.12

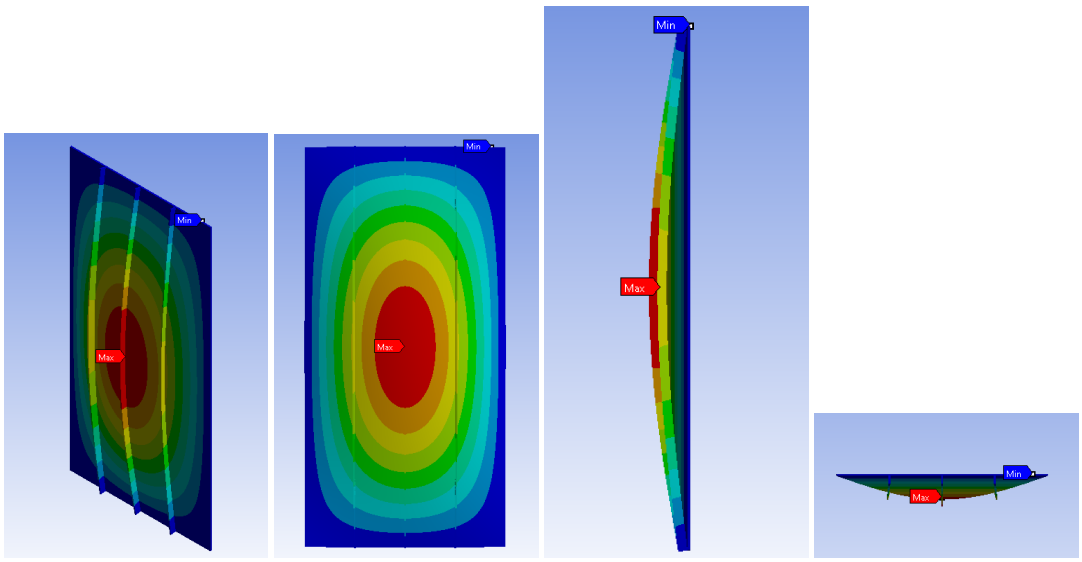

(a) Isometric View (b) Front view (c) Side View (d) Top View

Figure 4.11: Mode 1 (1,1) result of 3 box shaped stiffened plate (AISI 1090 Steel); N_{cr}= 1290.1 N/mm)

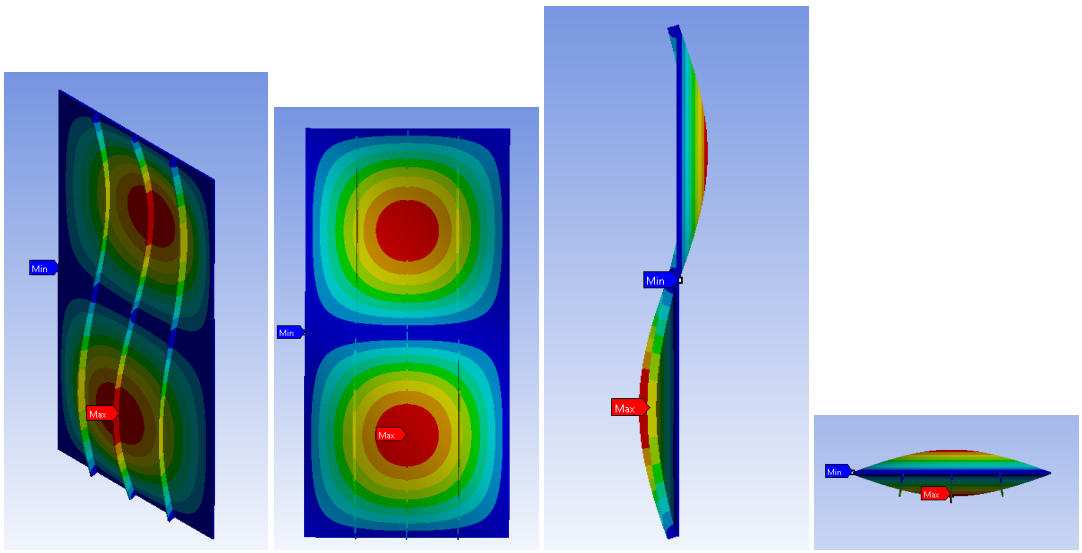

(a) Isometric View (b) Front view (c) Side View (d) Top View

Figure 4.12: Mode 2 (2,1) result of 3 box shaped stiffened plate (AISI 1090 Steel); N_{cr}= 1726.8 N/mm)

4.3.3 One L Shaped Stiffener

Plate Specification	
Length	2 m
Breadth	1 m
Thickness	0.01 m
Aspect Ratio (P)	2
AISI 1090 Steel	
Moment of Inertia (I)	0.0000002168004716 m^4
Flexural Stiffness (D)	18651.96
Sectional Area	0.0003425 m^2
Ratio of Bending Stiffness Rigidity of Stiffeners to the Plate (γ)	2.3828
Ratio of Cross Sectional Areas of the Stiffeners to the Plate (δ)	0.03425
Buckling Coefficient (K)	6.96
Critical Load (Theoretical)	1281.30 N/mm
Critical Load (Simulation)	1273.1 N/mm
Error Percentage	0.64%

Table 4.14: Theoretical Result of a rectangular plate with one L stiffener attached (AISI 1090 Steel)

Plate Specification	
Length	2 m
Breadth	1 m
Thickness	0.01 m
Aspect Ratio (P)	2
Mild Steel	
Moment of Inertia (I)	0.0000002168004716 m^4
Flexural Stiffness (D)	18315.02
Sectional Area	0.0003425 m^2
Ratio of Bending Stiffness Rigidity of Stiffeners to the Plate (γ)	2.368
Ratio of Cross Sectional Areas of the Stiffeners to the Plate (δ)	0.034
Buckling Coefficient (K)	6.95
Critical Load (Theoretical)	1256.87 N/mm
Critical Load (Simulation)	1248.6 N/mm
Error Percentage	0.66%

Table 4.15: Theoretical Result of a rectangular plate with one L stiffener attached (Mild Steel)

Plate Specification	
Length	2 m
Breadth	1 m
Thickness	0.01 m
Aspect Ratio (P)	2
Stainless Steel 302	
Moment of Inertia (I)	0.0000002168004716 m^4
Flexural Stiffness (D)	17155.56
Sectional Area	0.0003425 m^2
Ratio of Bending Stiffness Rigidity of Stiffeners to the Plate (γ)	2.439
Ratio of Cross Sectional Areas of the Stiffeners to the Plate (δ)	0.034
Buckling Coefficient (K)	6.986
Critical Load (Theoretical)	1182.933 N/mm
Critical Load (Simulation)	1176.2 N/mm
Error Percentage	0.57%

Table 4.16: Theoretical Result of a rectangular plate with one L stiffener attached (Stainless Steel 302)

Plate Specification	
Length	2 m
Breadth	1 m
Thickness	0.01 m
Aspect Ratio (P)	2
Stainless Steel 330	
Moment of Inertia (I)	0.0000002168004716 m^4
Flexural Stiffness (D)	17707.55
Sectional Area	0.0003425m^2
Ratio of Bending Stiffness Rigidity of Stiffeners to the Plate (γ)	2.412
Ratio of Cross Sectional Areas of the Stiffeners to the Plate (δ)	0.0343
Buckling Coefficient (K)	6.97
Critical Load (Theoretical)	1218.8 N/mm
Critical Load (Simulation)	1211.4 N/mm
Error Percentage	0.61%

Table 4.17: Theoretical Result of a rectangular plate with one L stiffener attached (Stainless Steel 330)

4.3.3.1 Simulation Results for One L Shaped Stiffener

The simulation results for one L shaped stiffener attached plate are shown as follows in Figure 4.13 and in Figure 4.14

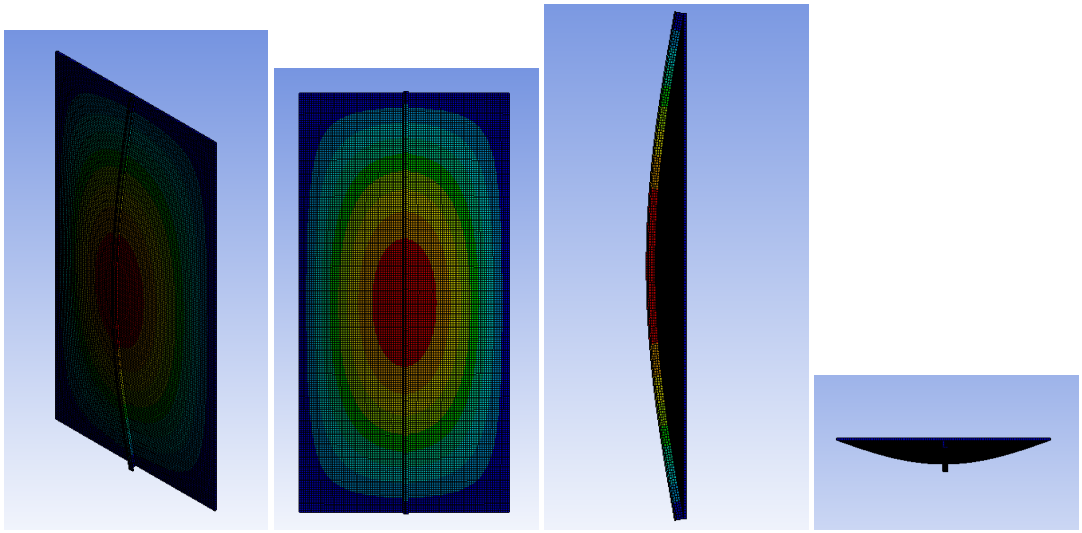

(a) Isometric View (b) Front view (c) Side View (d) Top View

Figure 4.13: Mode 1 (1,1) result of an L shaped stiffened plate (AISI 1090 Steel); N_{cr}= 1273.1 N/mm)

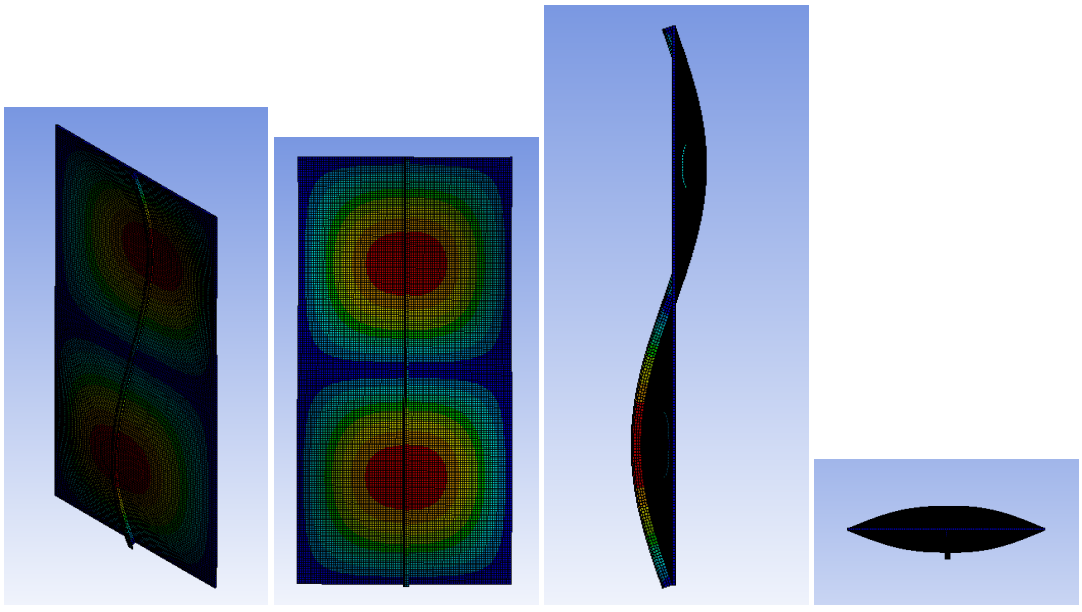

(a) Isometric View (b) Front view (c) Side View (d) Top View

Figure 4.14: Mode 2 (2,1) result of an L shaped stiffened plate (AISI 1090 Steel); N_{cr}= 1521 N/mm)

4.3.4 Three L Shaped Stiffener

Plate Specification	
Length	2 m
Breadth	1 m
Thickness	0.01 m
Aspect Ratio (P)	2
AISI 1090 Steel	
Moment of Inertia (I)	0.0000002168004716 m^4
Flexural Stiffness (D)	18651.96
Sectional Area	0.0003425 m^2
Ratio of Bending Stiffness Rigidity of Stiffeners to the Plate (γ)	2.3828
Ratio of Cross Sectional Areas of the Stiffeners to the Plate (δ)	0.03425
Buckling Coefficient (K)	7.63
Critical Load (Theoretical)	1404.76 N/mm
Critical Load (Simulation)	1409.1 N/mm
Error Percentage	0.31%

Table 4.18: Theoretical Result of a rectangular plate with three L stiffener attached (AISI 1090 Steel)

Plate Specification	
Length	2 m
Breadth	1 m
Thickness	0.01 m
Aspect Ratio (P)	2
Mild Steel	
Moment of Inertia (I)	0.0000002168004716 m^4
Flexural Stiffness (D)	18315.02
Sectional Area	0.0003425 m^2
Ratio of Bending Stiffness Rigidity of Stiffeners to the Plate (γ)	2.368
Ratio of Cross Sectional Areas of the Stiffeners to the Plate (δ)	0.034
Buckling Coefficient (K)	7.617
Critical Load (Theoretical)	1376.92 N/mm
Critical Load (Simulation)	1381.2 N/mm
Error Percentage	0.31%

Table 4.19: Theoretical Result of a rectangular plate with three L stiffener attached (Mild Steel)

Plate Specification	
Length	2 m
Breadth	1 m
Thickness	0.01 m
Aspect Ratio (P)	2
Stainless Steel 302	
Moment of Inertia (I)	0.0000002168004716 m^4
Flexural Stiffness (D)	17155.56
Sectional Area	0.0003425 m^2
Ratio of Bending Stiffness Rigidity of Stiffeners to the Plate (γ)	2.439
Ratio of Cross Sectional Areas of the Stiffeners to the Plate (δ)	0.034
Buckling Coefficient (K)	7.68
Critical Load (Theoretical)	1300.47 N/mm
Critical Load (Simulation)	1304.2 N/mm
Error Percentage	0.29%

Table 4.20: Theoretical Result of a rectangular plate with three L stiffener attached (Stainless Steel 302)

Plate Specification	
Length	2 m
Breadth	1 m
Thickness	0.01 m
Aspect Ratio (P)	2
Stainless Steel 330	
Moment of Inertia (I)	0.0000002168004716 m^4
Flexural Stiffness (D)	17707.55
Sectional Area	0.0003425m^2
Ratio of Bending Stiffness Rigidity of Stiffeners to the Plate (γ)	2.412
Ratio of Cross Sectional Areas of the Stiffeners to the Plate (δ)	0.0343
Buckling Coefficient (K)	7.66
Critical Load (Theoretical)	1338.137 N/mm
Critical Load (Simulation)	1342.1 N/mm
Error Percentage	0.30%

Table 4.21: Theoretical Result of a rectangular plate with three L stiffener attached (Stainless Steel 330)

4.3.4.1 Simulation Results for Three L Shaped Stiffeners

The simulation results for three L shaped stiffeners attached plate are shown as follows in Figure 4.15 and in Figure 4.16

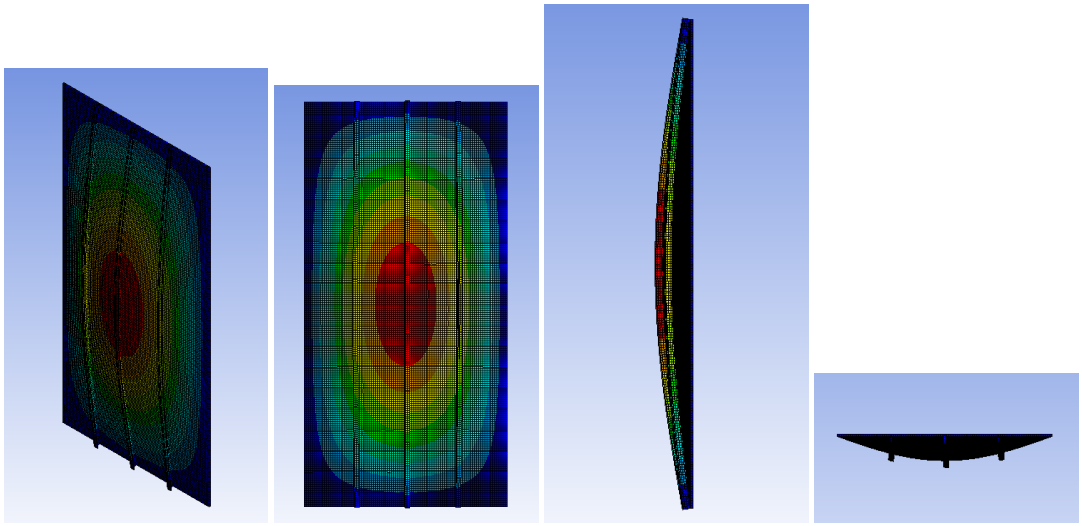

(a) Isometric View (b) Front view (c) Side View (d) Top View

Figure 4.15: Mode 1 (1,1) result of three L shaped stiffened plate (AISI 1090 Steel); N_{cr}= 1409.1 N/mm)

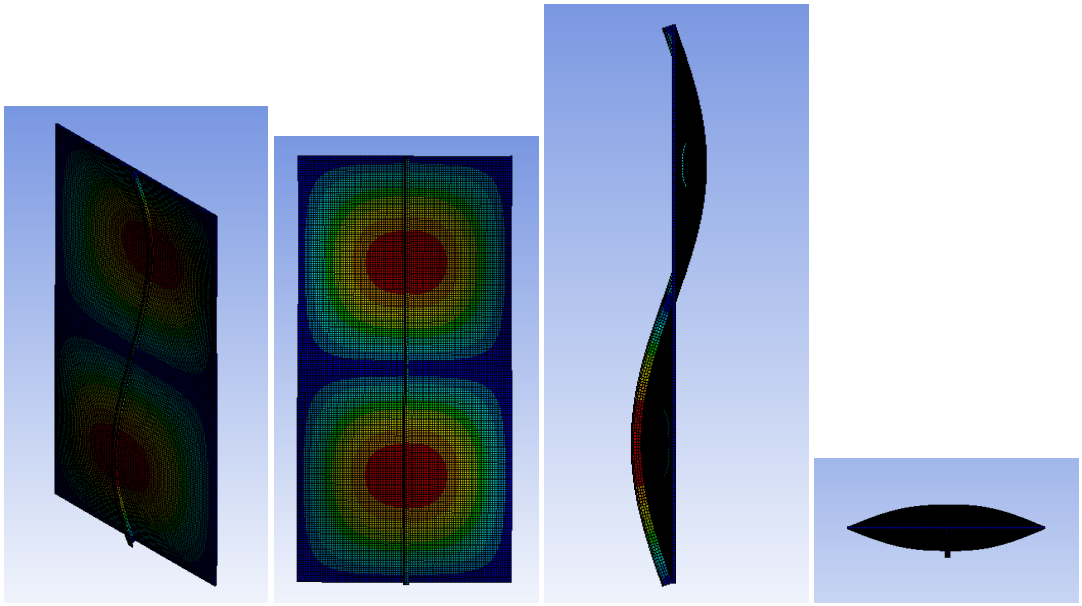

(a) Isometric View (b) Front view (c) Side View (d) Top View

Figure 4.16: Mode 2 (2,1) result of three L shaped stiffened plate (AISI 1090 Steel); N_{cr}= 2014.6 N/mm)

4.3.5 One T Shaped Stiffener

Plate Specification	
Length	2 m
Breadth	1 m
Thickness	0.01 m
Aspect Ratio (P)	2
AISI 1090 Steel	
Moment of Inertia (I)	0.0000003329195 m^4
Flexural Stiffness (D)	18651.96
Sectional Area	0.0004185 m^2
Ratio of Bending Stiffness Rigidity of Stiffeners to the Plate (γ)	3.659
Ratio of Cross Sectional Areas of the Stiffeners to the Plate (δ)	0.042
Buckling Coefficient (K)	7.45
Critical Load (Theoretical)	1371.203 N/mm
Critical Load (Simulation)	1395 N/mm
Error Percentage	1.74%

Table 4.22: Theoretical Result of a rectangular plate with one T stiffener attached (AISI 1090 Steel)

Plate Specification	
Length	2 m
Breadth	1 m
Thickness	0.01 m
Aspect Ratio (P)	2
Mild Steel	
Moment of Inertia (I)	0.0000003329195 m^4
Flexural Stiffness (D)	18315.02
Sectional Area	0.0004185 m^2
Ratio of Bending Stiffness Rigidity of Stiffeners to the Plate (γ)	3.636
Ratio of Cross Sectional Areas of the Stiffeners to the Plate (δ)	0.042
Buckling Coefficient (K)	7.44
Critical Load (Theoretical)	1344.478 N/mm
Critical Load (Simulation)	1367.4 N/mm
Error Percentage	1.70%

Table 4.23: Theoretical Result of a rectangular plate with one T stiffener attached (Mild Steel)

Plate Specification	
Length	2 m
Breadth	1 m
Thickness	0.01 m
Aspect Ratio (P)	2
Stainless Steel 302	
Moment of Inertia (I)	0.0000003329195 m^4
Flexural Stiffness (D)	17155.56
Sectional Area	0.0004185 m^2
Ratio of Bending Stiffness Rigidity of Stiffeners to the Plate (γ)	3.745
Ratio of Cross Sectional Areas of the Stiffeners to the Plate (δ)	0.042
Buckling Coefficient (K)	7.49
Critical Load (Theoretical)	1267.9 N/mm
Critical Load (Simulation)	1291.2 N/mm
Error Percentage	1.84%

Table 4.24: Theoretical Result of a rectangular plate with one T stiffener attached (Stainless Steel 302)

Plate Specification	
Length	2 m
Breadth	1 m
Thickness	0.01 m
Aspect Ratio (P)	2
Stainless Steel 330	
Moment of Inertia (I)	0.0000003329195 m^4
Flexural Stiffness (D)	17707.55
Sectional Area	0.0004185m^2
Ratio of Bending Stiffness Rigidity of Stiffeners to the Plate (γ)	3.70
Ratio of Cross Sectional Areas of the Stiffeners to the Plate (δ)	0.042
Buckling Coefficient (K)	7.47
Critical Load (Theoretical)	1305.36 N/mm
Critical Load (Simulation)	1328.7 N/mm
Error Percentage	1.79%

Table 4.25: Theoretical Result of a rectangular plate with one T stiffener attached (Stainless Steel 330)

4.3.5.1 Simulation Results for One T Shaped Stiffener

The simulation results for one T shaped stiffener attached plate are shown as follows in Figure 4.17 and in Figure 4.18

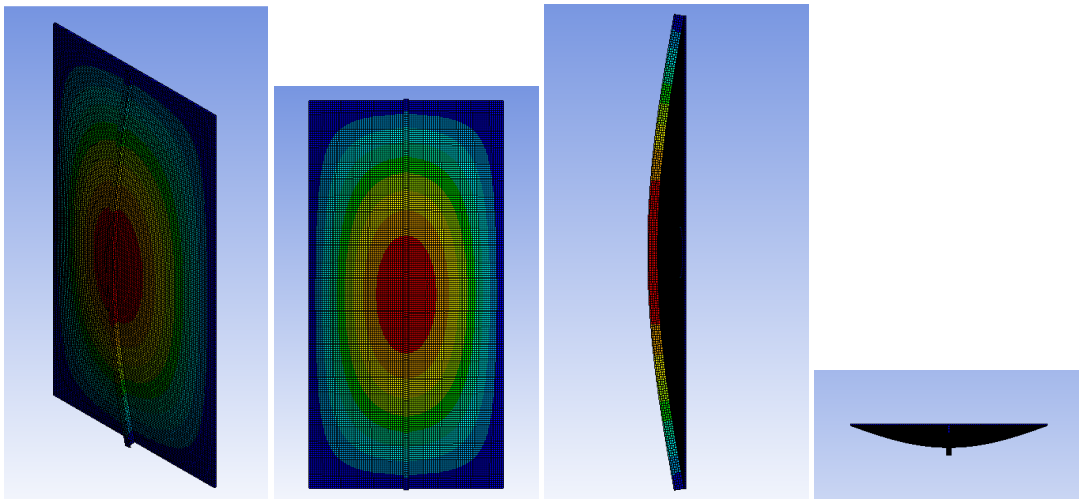

(a) Isometric View (b) Front view (c) Side View (d) Top View

Figure 4.17: Mode 1 (1,1) result of one T shaped stiffened plate (AISI 1090 Steel); N_{cr}= 1395 N/mm)

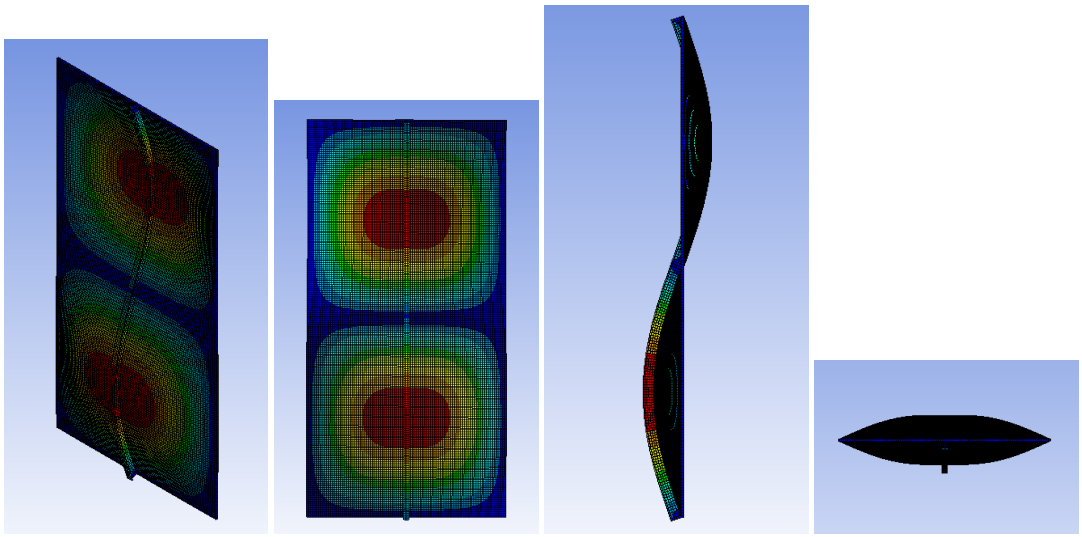

(a) Isometric View (b) Front view (c) Side View (d) Top View

Figure 4.18: Mode 2 (2,1) result of one T shaped stiffened plate (AISI 1090 Steel); N_{cr}= 1961.5 N/mm)

4.3.6 Three T Shaped Stiffeners

Plate Specification	
Length	2 m
Breadth	1 m
Thickness	0.01 m
Aspect Ratio (P)	2
AISI 1090 Steel	
Moment of Inertia (I)	0.0000003329195 m^4
Flexural Stiffness (D)	18651.96
Sectional Area	0.0004185 m^2
Ratio of Bending Stiffness Rigidity of Stiffeners to the Plate (γ)	3.659
Ratio of Cross Sectional Areas of the Stiffeners to the Plate (δ)	0.042
Buckling Coefficient (K)	8.54
Critical Load (Theoretical)	1572.02 N/mm
Critical Load (Simulation)	1613.1 N/mm
Error Percentage	2.61%

Table 4.26: Theoretical Result of a rectangular plate with Three T stiffener attached (AISI 1090 Steel)

Plate Specification	
Length	2 m
Breadth	1 m
Thickness	0.01 m
Aspect Ratio (P)	2
Mild Steel	
Moment of Inertia (I)	0.0000003329195 m^4
Flexural Stiffness (D)	18315.02
Sectional Area	0.0004185 m^2
Ratio of Bending Stiffness Rigidity of Stiffeners to the Plate (γ)	3.636
Ratio of Cross Sectional Areas of the Stiffeners to the Plate (δ)	0.042
Buckling Coefficient (K)	8.52
Critical Load (Theoretical)	1539.95 N/mm
Critical Load (Simulation)	1578.5 N/mm
Error Percentage	2.50%

Table 4.27: Theoretical Result of a rectangular plate with Three T stiffener attached (Mild Steel)

Plate Specification	
Length	2 m
Breadth	1 m
Thickness	0.01 m
Aspect Ratio (P)	2
Stainless Steel 302	
Moment of Inertia (I)	0.0000003329195 m^4
Flexural Stiffness (D)	17155.56
Sectional Area	0.0004185 m^2
Ratio of Bending Stiffness Rigidity of Stiffeners to the Plate (γ)	3.745
Ratio of Cross Sectional Areas of the Stiffeners to the Plate (δ)	0.042
Buckling Coefficient (K)	8.61
Critical Load (Theoretical)	1458.50 N/mm
Critical Load (Simulation)	1502.6 N/mm
Error Percentage	3.02%

Table 4.28: Theoretical Result of a rectangular plate with Three T stiffener attached (Stainless Steel 302)

Plate Specification	
Length	2 m
Breadth	1 m
Thickness	0.01 m
Aspect Ratio (P)	2
Stainless Steel 330	
Moment of Inertia (I)	0.0000003329195 m^4
Flexural Stiffness (D)	17707.55
Sectional Area	0.0004185m^2
Ratio of Bending Stiffness Rigidity of Stiffeners to the Plate (γ)	3.70
Ratio of Cross Sectional Areas of the Stiffeners to the Plate (δ)	0.042
Buckling Coefficient (K)	8.58
Critical Load (Theoretical)	1499.17 N/mm
Critical Load (Simulation)	1471.3 N/mm
Error Percentage	1.86%

Table 4.29: Theoretical Result of a rectangular plate with Three T stiffener attached (Stainless Steel 330)

4.3.6.1 Simulation Results for Three T Shaped Stiffener

The simulation results for three T shaped stiffeners attached plate are shown as follows in Figure 4.19 and in Figure 4.20

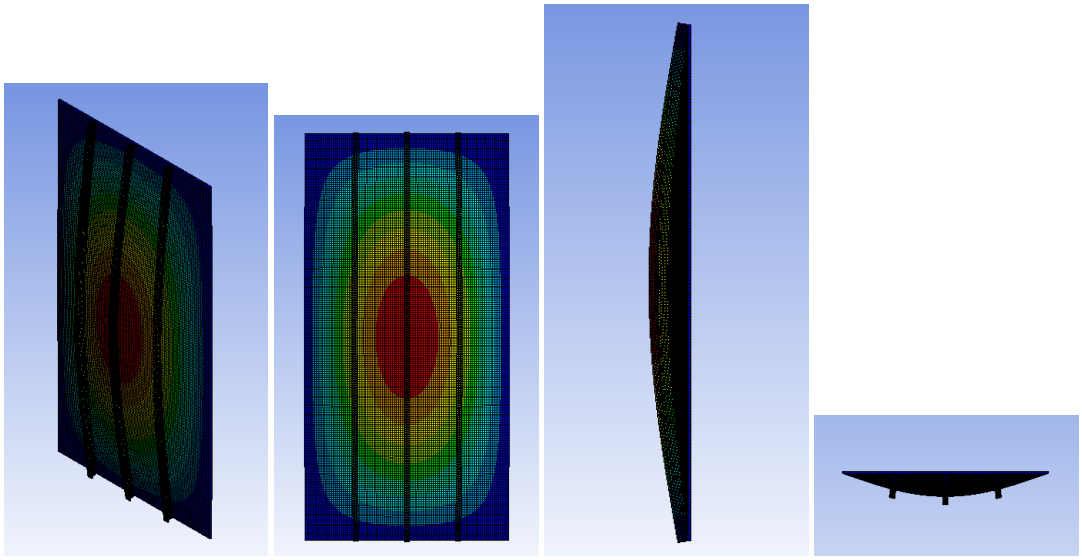

(a) Isometric View (b) Front view (c) Side View (d) Top View

Figure 4.19: Mode 1 (1,1) result of three T shaped stiffened plate (AISI 1090 Steel); N_{cr}= 1574.4 N/mm)

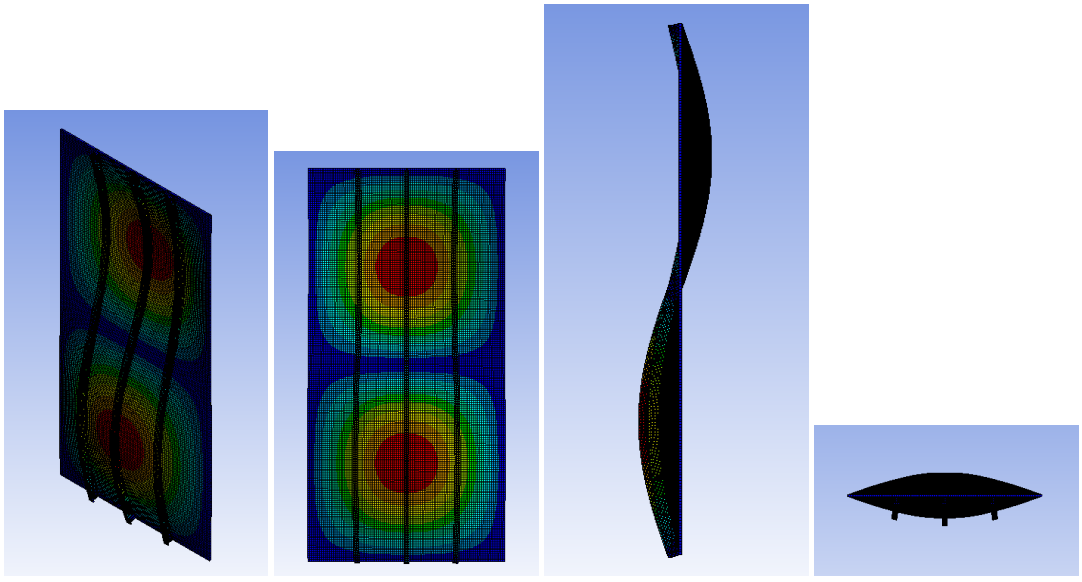

(a) Isometric View (b) Front view (c) Side View (d) Top View

Figure 4.20: Mode 2 (2,1) result of three T shaped stiffened plate (AISI 1090 Steel); N_{cr}= 3039.4 N/mm)

4.4 Stress Development analysis in different region under Buckling Load

When a plate is subject to an in-plane axial load, Buckling of the structure will occur under its critical load. The mode of the buckle may vary depending on the structural geometry or aspect ratio of the stiffened panel. In response to the buckling load, different regions of the plate may experience deformation stress during the buckling process. The corresponding value is taken after running simulation for different boundary condition, described in Table 4.30.

Material Type	For SSSS Condition		For CCCC Condition	
	Critical Load (MPa)	Stress Development (MPa)	Critical Load (MPa)	Stress Development (MPa)
AISI 1090 Steel	73.635	73.635	1448.7	144.87
Mild Steel	72.304	72.304	1421.6	142.16
Stainless Steel 302	67.729	67.729	1331.8	133.18
Stainless Steel 330	69.907	69.907	1374.5	137.45

Table 4.30: Stress development on flat plate without attaching any stiffener

4.4.1 Stress development under simply supported Rectangular stiffened plate in all four edges

Similar process is carried out for stiffened rectangle plate where a rectangular plate is attached to one and three box, L and T shaped stiffener as shown in Figure 4.21.

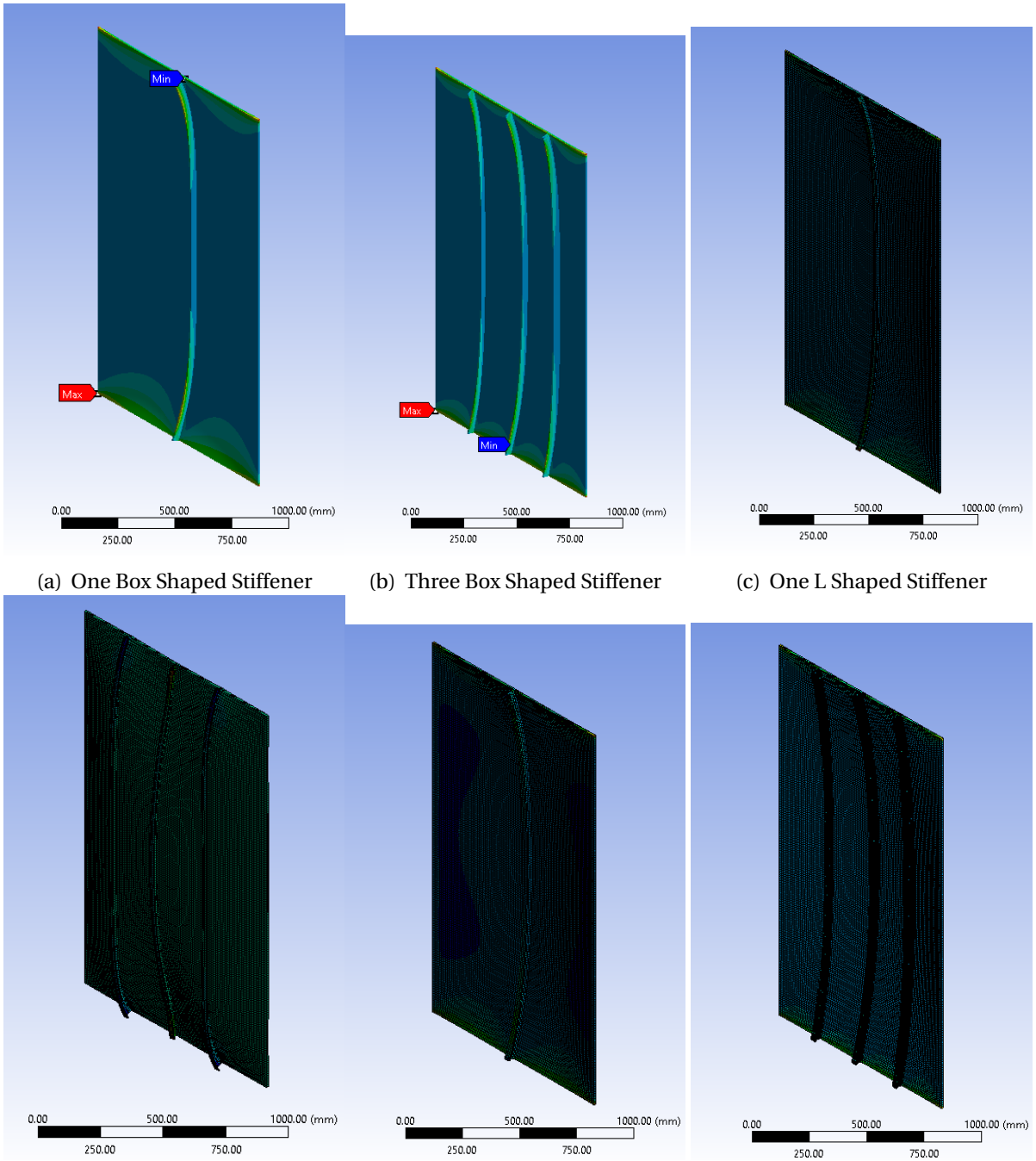

(a) One Box Shaped Stiffener (b) Three Box Shaped Stiffener (c) One L Shaped Stiffener

(d) Three L Shaped Stiffener (e) One T Shaped Stiffener (f) Three T Shaped Stiffener

Figure 4.21: Stress development for stiffened panel in SSSS condition

And the corresponding simulation results are as follows:

Material Type	Stiffener Type	Critical Load (Mpa)	Equivalent Stress (MPa)		
			Min	Max	Avg
AISI 1090 Steel	Box Shaped	1222.2	10.283	807.82	147.9
	L Shaped	1273.1	11.793	967.27	160.14
	T Shaped	1395	38.921	922.32	170.59
Mild Steel	Box Shaped	1199.2	8.9352	782.51	145.07
	L Shaped	1248.6	11.259	948.72	156.99
	T Shaped	1367.4	36.603	902.39	167.16
Stainless Steel 302	Box Shaped	1127.6	10.693	783.4	136.67
	L Shaped	1176.2	13.156	894.13	148.23
	T Shaped	1291.2	38.762	881.09	158.15
Stainless Steel 330	Box Shaped	1162.1	11.327	787.72	140.73
	L Shaped	1211.4	12.192	920.49	152.52
	T Shaped	1328.7	39.87	884.69	162.61

Table 4.31: Stress development on one stiffened rectangular plate.

Material Type	Stiffener Type	Critical Load (Mpa)	Equivalent Stress (MPa)		
			Min	Max	Avg
AISI 1090 Steel	Box Shaped	1290.1	14.271	770.87	150.71
	L Shaped	1409.1	3.55	376.2	133.98
	T Shaped	1574.4	11.54	1041.7	212.57
Mild Steel	Box Shaped	1264.9	14.519	746.48	147.73
	L Shaped	1381.2	3.5223	368.67	131.33
	T Shaped	1541.7	10.635	1018.2	208.04
Stainless Steel 302	Box Shaped	1193.3	11.92	748.34	139.58
	L Shaped	1304.2	3.1343	348.52	124
	T Shaped	1462.9	14.726	975.4	197.93
Stainless Steel 330	Box Shaped	1228.3	12.776	752.1	143.58
	L Shaped	1342.1	3.3014	358.48	127.6
	T Shaped	1502.6	12.846	997.91	203.09

Table 4.32: Stress development on three stiffened rectangular plate.

CHAPTER 5

COMPARATIVE ANALYSIS

5.1 Comparison of Critical Buckling Load

Critical Buckling Loads (N/mm)							
Simply Supported Plate (SSSS)	Clamped Plate (CCCC)	Stiffened Plate					
		Box Shaped		L Shaped		T shaped	
		1 Box Shaped Stiffened Plate	3 Box Shaped Stiffened Plate	1 L shaped Stiffened Plate	3 L shaped Stiffened Plate	1 T shaped Stiffened Plate	3 T shaped Stiffened Plate
AISI 1090 Steel							
736.35	1448.7	1222.2	1290.1	1273.1	1409.1	1395	1574.4
Mild Steel							
723.04	1428.03	1199.2	1264.9	1248.6	1381.2	1367.4	1541.7
Stainless Steel 302							
677.29	1337.62	1127.6	1193.3	1176.2	1304.2	1291.2	1462.9
Stainless Steel 330							
699.07	1380.66	1162.1	1228.3	1211.4	1342.1	1328.7	1502.6

From the above table, we can see that the material AISI steel has the highest critical buckling load for all cases. The effect of boundary conditions on the plates is an important factor. When the boundary condition changed from SSSS to CCCC., the critical buckling load has increased from 736.35 to 1448.7 for AISI 1090 Steel which is about an increase of 96.7% which is about double of the previous value. For stiffened plates, the increase in the number of stiffeners increases the critical buckling load for all stiffeners. The increase in critical load for one box, one L and one T shaped stiffeners compared to a base plate subject to buckling at simply supported boundary condition is 65.98%, 72.89% and 89.45%. Out of the three types of stiffeners, the T shaped stiffener has a better buckling resistance. Another observation is that, except 3 T shaped stiffeners attached to a plate, all the other stiffened plates give a

critical load less than that of a unstiffened plate under clamped boundary condition. This states the effect of boundary condition on the buckling behaviour of a plate.

CHAPTER 6

CONCLUSION

Buckling of a structure and its first mode of deformation is required to be found to predict the value of the critical buckling load under which a plate may start to buckle. Linear buckling analysis predicts only the buckled shape, not the direction in which it deforms. In our study, we tried to analyse how a plate reacts to axial load under 2 different boundary conditions. Among these two boundary conditions (All edges simply supported and all edges clamped), the buckling resistance in case of clamped edges is more than simply supported edges. That means it can resist more amount of loads based on its boundary condition.

In case of buckling of a simply supported flat plate (SSSS) the aspect ratio of a plate does not have any effect on the critical buckling coefficient. So with the change in the aspect ratio of a plate, the number of half waves along the length, that is the value of m changes keeping the critical load constant. This states that the mode of deformation of the plate will be different for plates with different aspect ratios under the SSSS boundary condition. But in case of CCCC boundary condition, the critical buckling coefficient will change with the change in plate aspect ratios.This can be understood well from the Figure 2.8 and Figure 2.9

Stiffeners are used as an alternative to increase plate thickness to resist higher amount of loads by intermediate members attached. The stiffener shape and their moment of Inertia is an important factor to resist the buckling loads. Among the stiffeners used, the T shaped stiffener comparatively resists buckling better than L and Box shaped stiffeners. It is because in a T shaped stiffener, the moment of inertia gain is more than the other shapes because of its weight distribution.

With the increase in the number of stiffeners, the critical buckling load increases. The highest critical buckling load is given by three T shape stiffeners attached to a plate in all the studies done in this thesis.

The effect of boundary condition sometimes increases the buckling capacity of structure regardless of stiffeners attached to a plate. For instance, a simple plate under clamped boundary condition can resist more axial forces than a simply supported plate having one stiffener.

Material Property is an important factor in resisting buckling. Among the different types of steel analyzed, the AISI 1090 Steel outperforms the other materials in both stiffened and unstiffened conditions.

For unstiffened rectangular flat plates in both SSSS and CCCC boundary conditions, the developed equivalent (von mises) stresses against the critical buckling load is significantly less than the yield stress of the materials. So, buckling mode of failure will occur before other modes of failure such as yielding.

For the stiffened plates under SSSS boundary conditions, the maximum von mises stress developed at corner points along the edges exceed the yield stress limit value but the average local stress at the location where the maximum critical buckling load is found is below the yield stress limit. So, buckling will occur before yielding in that region and the buckling load will cause plastic deformation on the regions where the local stress exceeds the yield stress.

REFERENCES

[1] MS Windows NT kernel description. https://ocw.mit.edu/courses/2-080j-structural-mechanics-fall-2013/resources/mit2_080jf13_lecture11/. Accessed: 2010-09-30.

[2] Bedair, O. K. (1998). A contribution to the stability of stiffened plates under uniform compression. *Computers & structures*, 66(5):535–570.

[3] Cox, H. (1954). Computation of initial buckling stress for sheet-stiffener combinations. *The Aeronautical Journal*, 58(525):634–638.

[4] Guyon, Y. (1946). Calcul des ponts larges a poutres multiples solidarisees par les entretoises. In *Annales des Ponts et Chaussees*, volume 24, page 553.

[5] Hassan, A. H. A. and Kurgan, N. (2019). Modeling and buckling analysis of rectangular plates in ansys. *International Journal of Engineering and Applied Sciences*, 11(1):310–329.

[6] Hovichitr, I., SL, L., et al. (1977). A rational analysis of plates with eccentric stiffeners.

[7] Ibearugbulem, M., Ibeabuchi, V., and Njoku, K. (2014). Buckling analysis of ssss stiffened rectangular isotropic plates using work principle approach. *International Journal of Innovative Research & Development*, 3(11):169–176.

[8] Klitchieff, J. (1949). On the stability of plates reinforced by ribs.

[9] Kumar, P. R., Gupta, G., Shamili, G., and Anitha, D. (2018). Linear buckling analysis and comparative study of un-stiffened and stiffened composite plate. *Materials Today: Proceedings*, 5(2):6059–6071.

[10] Maaskant, R. (1990). Interactive buckling of biaxially loaded elastic plate structures.

[11] Martin, D. and Cox, H. (1963). The buckling modes of a longitudinally stiffened flat panel. *Aeronautical Quarterly*, 14(4):396–398.

[12] Massonnet, C. (1950). Methods de calcul des points a poutres multiples tenant compte de leur resistance a la torsion. *Proc. Int. Association for Bridge and Structural Engineering*, 10:147–182.

[13] Shama, M. (2012). *Buckling of ship structures*. Springer Science & Business Media.

[14] Singh, A. (2013). *Analysis of stiffened rectangular plate.* PhD thesis.

[15] Soper, W. (1958). Large deflection of stiffened plates.